Occurrence of Bacterial Membrane Microdomain at the Cell Division Site Enriched in Phospholipids with Polyunsaturated Hydrocarbon Chain*

Sho Sato[1,2], Jun Kawamoto[1], Satoshi B. Sato[3], Bunta Watanabe[1], Jun Hiratake[1], Nobuyoshi Esaki[1], and Tatsuo Kurihara[1]

[1]Institute for Chemical Research, Kyoto University, Uji, Kyoto 611-0011, Japan
[2]Research Fellow of the Japan Society for the Promotion of Science
[3]Research Center for Low Temperature and Material Sciences, Kyoto University, Kyoto 606-8501, Japan

*Running title: *Bacterial membrane microdomain at the cell division site*

To whom corresponding should be addressed: Tatsuo Kurihara, Institute for Chemical Research, Kyoto University, Uji, Kyoto 611-0011, Japan, Tel.: +81-774-38-4710; Fax: +81-774-38-3248; E-mail: kurihara@scl.kyoto-u.ac.jp

Keywords: membrane microdomain; polyunsaturated fatty acid; eicosapentaenoic acid

Background: Phospholipids containing polyunsaturated hydrocarbon chain play important roles in various biological membranes.
Results: Fluorescence microscopic analysis with a chemically synthesized fluorescent probe showed localization of phospholipids containing an eicosapentaenyl group at the bacterial cell division site.
Conclusion: Phospholipids containing polyunsaturated hydrocarbon chain form a membrane microdomain at the cell center to promote cell division.
Significance: Hydrocarbon-chain-dependent microdomain formation was visualized *in vivo*.

SUMMARY

We found in this study that phospholipids containing an eicosapentaenyl group form a novel membrane microdomain at the cell division site of a Gram-negative bacterium, *Shewanella livingstonensis* Ac10, by using chemically synthesized fluorescent probes. The occurrence of membrane microdomains in eukaryotes and prokaryotes has been demonstrated with various imaging tools for phospholipids with different polar head groups. However, little has been studied regarding hydrocarbon-chain-dependent localization of membrane-resident phospholipids *in vivo*. We previously found that lack of eicosapentaenoic acid (EPA), a polyunsaturated fatty acid found at the *sn*-2 position of glycerophospholipids, causes a defect in cell division after DNA replication of *S. livingstonensis* Ac10. Here, we synthesized phospholipid probes labeled with a fluorescent 7-nitro-2,1,3-benzoxadiazol-4-yl (NBD) group to study the localization of EPA-containing phospholipids by fluorescence microscopy. A fluorescent probe, in which EPA is bound to the glycerol backbone via an ester bond, was found to be unsuitable for imaging because EPA was released from the probe by *in vivo* hydrolysis. To overcome this problem, we synthesized hydrolysis-resistant ether-type phospholipid probes. Using these probes, we found that the fluorescence localized between two nucleoids at the cell center during cell division when the cells were grown in the presence of the eicosapentaenyl-group-containing probe (*N*-NBD-1-oleoyl-2-eicosapentaenyl-*sn*-glycero-3-phosphoethanolamine), whereas this localization was not observed with the oleyl-group-containing control probe (*N*-NBD-1-oleoyl-2-oleyl-*sn*-glycero-3-phosphoethanolamine). Thus, phospholipids containing an eicosapentaenyl group are specifically enriched at the cell division site. Formation of a membrane microdomain enriched in EPA-containing phospholipids at the nucleoid occlusion site probably facilitates cell division.

Biological membranes are composed of lipids and proteins and play essential roles in all living organisms in nutrient uptake, waste efflux, signal transduction, morphogenesis, etc. According to the fluid mosaic model proposed by Singer and Nicolson (1), it was previously assumed that lipids are homogeneously

distributed in biological membranes. However, this view was considerably modified by the discovery of membrane microdomains, each of which is supposed to have specific physiological functions.

Various lipid molecules form membrane microdomains in eukaryotes and prokaryotes. Eukaryotic cells contain membrane microdomains, known as lipid rafts, that are enriched in sphingolipids and sterols (2). Lipid rafts serve as platforms for the colocalization of proteins involved in signaling and transport. In prokaryotes, cardiolipin microdomains exist at the poles and septa in the rod-shaped cells of *Escherichia coli*, *Bacillus subtilis*, and *Pseudomonas putida* (3, 4). Recently, the membrane of *B. subtilis* was reported to contain microdomains functionally similar to the lipid rafts of eukaryotic cells (5). These observations indicate the importance of dissecting the distribution of individual lipid molecules in biological membranes to better understand the mechanisms behind biological phenomena observed at the cell membrane.

Long-chain ω-3 polyunsaturated fatty acids, eicosapentaenoic acid (EPA, 20:5 $_{5,8,11,14,17\ \text{all cis}}$) and docosahexaenoic acid (DHA, 22:6 $_{4,7,10,13,16,19\ \text{all cis}}$), have been attracting a great deal of attention mainly because of their beneficial effects on human health (6-8). EPA and DHA occur in the membranes of various organisms, including mammals and bacteria, as acyl chains of phospholipids. EPA and DHA serve as precursors of various eicosanoids and autacoids (9). DHA interacts with membrane-associated G protein-coupled receptors to support their function (10-12). In EPA-producing bacteria, EPA plays a beneficial role in cell division (13, 14). However, the molecular mechanisms of EPA and DHA action are not well defined, in particular, their roles in coordinating the spatial organization of the phospholipids that contain them in biological membranes.

A Gram-negative bacterium, *Shewanella livingstonensis* Ac10, which produces EPA as an *sn*-2 acyl chain of phosphatidylethanolamine (PE) and phosphatidylglycerol (PG) (13, 15), is an excellent model organism for the studies on *in vivo* EPA function because of the following (13, 15-17): (i) The genes coding for EPA synthase are known, enabling the construction of an EPA-less mutant by disruption of these genes. (ii) The phenotype of the EPA-less mutant is clear; depletion of EPA causes growth retardation at low temperatures and produces filamentous cells because of a defect in cell division. (iii) The structure-function relationship of EPA can be studied by externally adding a series of EPA analogs to the culture medium. (iv) The whole genome sequence is available for this bacterium. (v) The methods for the genetic manipulation of this bacterium have been established. (vi) As a bacterium, it has a much simpler membrane system than eukaryotic cells.

To gain more insight into the function of the EPA-containing phospholipids in the cell membrane, we synthesized fluorescent molecular probes in this study to visualize the distribution of phospholipids containing polyunsaturated hydrocarbon chains. Recently, advances in the methods for labeling small molecules to visualize their subcellular localization have been made. For phospholipids, methods have been reported for visualization of phosphatidylserine (18), phosphatidylethanolamine (19), phosphatidylcholine (20, 21), phosphatidic acid (22), and sphingomyelin (21, 23). However, hydrocarbon chain-dependent localization of phospholipids cannot be visualized by using currently available molecular probes. To achieve this, we introduced a fluorescent group into the head group of phospholipids. A polyunsaturated hydrocarbon chain was bound to the phospholipids via an ether bond (an ester bond did not work because it was hydrolyzed in *S. livingstonensis* Ac10, resulting in the release of the polyunsaturated hydrocarbon chain from the probe molecule). By using this fluorescent probe, we found that phospholipids with an eicosapentaenyl group are enriched at the cell division site of *S. livingstonensis* Ac10. This is in accordance with the physiological function of EPA-containing phospholipids in the cell division of this bacterium. These results greatly contribute to understanding the *in vivo* function of polyunsaturated fatty acids and indicate the usefulness of the probe we synthesized.

EXPERIMENTAL PROCEDURES

Synthesis of fluorescent phospholipid probes -- 7-Nitro-2,1,3-benzoxadiazol-4-yl (NBD)-labeled phospholipids shown in Fig. 1 were chemically synthesized according to the methods described in Supplemental Data.

Bacterial strain and growth conditions -- The EPA-less mutant of *S. livingstonensis* Ac10 used in this study was constructed by the disruption of *orf5*, one of the genes required for EPA synthesis (13). We previously found that

this EPA-less mutant is longer than the wild-type strain because of retardation of cell division after DNA replication; this longer bacterial length facilitates microscopic analysis of the phospholipid subcellular localization, as fluorescence microscopic analysis of the much shorter wild-type strain cells is difficult. The cells were grown in LB medium containing 50 μg ml^{-1} rifampicin and 40 μg ml^{-1} kanamycin for 48 h at 18°C. The seed culture was used to inoculate 5 ml of LB medium containing 0.13 mM of the various NBD-labeled phospholipids chemically synthesized in this study. The phospholipid solution in chloroform was dried in a sterilized tube with nitrogen gas, resolubilized in 80 μl of ethanol, and then hydrated with 5 ml of LB medium to a final concentration of 0.13 mM by vortexing. The cells were cultured at 6°C for 250 h until they reached stationary phase.

Fluorescence microscopic analysis -- The culture (100 μl each) was sampled at 150, 200, and 250 h, and the fluorescence images were obtained using an epifluorescence microscope. For nuclei labeling, the cells collected at 250 h were treated with Hoechst 33342 (final concentration = 25 μg/ml) and washed twice with 200 μl of buffer A (0.75 M sucrose, 10 mM Tris-HCl (pH 7.5)). The fluorescence images were also obtained after dithionite treatment of the cells to quench the NBD fluorescence in the outer leaflet of the outer membrane. Further details are described in Supplemental Data.

ESI-MS analysis of phospholipids -- After fluorescence microscopic analysis, lipids were extracted from the residual sample by the Bligh and Dyer method (24) and analyzed by electrospray ionization mass spectrometry (ESI-MS). Details of the ESI-MS analysis are described in Supplemental Data.

Dithionite assay for measuring lipid distribution in the inner membrane (IM) and outer membrane (OM) -- To determine the distribution of NBD-labeled phospholipids in the IM and OM of the bacterium, we employed a fluorescence-quenching assay by using sodium dithionite. For this assay, the following three samples were prepared: non-treated, lysozyme-treated, and lysozyme-and-Triton X-100-treated cells (Fig. S1A). In the non-treated samples, only NBD-labeled phospholipids at the outer leaflet of the OM (OM_{out}) are accessible by dithionite, and their fluorescence is quenched. In the lysozyme-treated samples, the OM is disrupted, and both the inner leaflet of the OM (OM_{in}) and the outer leaflet of the IM (IM_{out}), in addition to the OM_{out}, become accessible to dithionite for fluorescence quenching. In the lysozyme-and-Triton X-100-treated samples, both OM and IM are disrupted, and the inner leaflet of the IM (IM_{in}), as well as the OM_{out}, OM_{in}, and IM_{out}, become accessible to dithionite. Further details of the dithionite assay are described in Supplemental Data.

RESULTS

Fate of fluorescence-labeled diacyl phospholipids in the cell membranes -- To visualize EPA-containing phospholipids in *S. livingstonensis* Ac10, we first synthesized a fluorescence-labeled phospholipid, *N*-NBD-1-oleoyl-2-eicosapentaenoyl-*sn*-glycero-3-phosphoethanolamine (Diacyl-EPA) (Fig. 1 and Supplemental Data for the synthesis). EPA was introduced into the *sn*-2 position because a polyunsaturated fatty acid is primarily found at this position in phospholipids in *S. livingstonensis* Ac10 and other organisms (25). The fluorescent NBD group was introduced into the head group to avoid modification of the hydrocarbon chain, which is to be characterized in the present study. As a control, we synthesized *N*-NBD-1,2-dioleoyl-*sn*-glycero-3-phosphoethanolamine (Diacyl-OLA), which contains the oleoyl group instead of the eicosapentaenoyl group at the *sn*-2 position (Fig. 1 and Supplemental Data for the synthesis). In these phospholipids, oleic acid (OLA, $18{:}1_{9cis}$) was introduced into the *sn*-1 position, because OLA and OLA-containing phospholipids were shown to have neutral effects on the phenotype of the EPA-less mutant (13, 15).

S. livingstonensis Ac10 was grown at 6°C in LB medium supplemented with Diacyl-EPA or Diacyl-OLA, and the cellular phospholipids were analyzed by ESI-MS. We found that the amounts of Diacyl-EPA and Diacyl-OLA in cellular membranes gradually decreased during cultivation for 166 h, while PEs and PGs containing EPA or OLA gradually increased (Fig. S2). The results suggest that Diacyl-EPA and Diacyl-OLA were hydrolyzed to yield free fatty acids, which were then incorporated into cellular PEs and PGs. Outer membrane phospholipase A likely catalyzed this hydrolysis (15, 26, 27). The NBD-moiety of Diacyl-EPA and Diacyl-OLA was not introduced into cellular phospholipids, as evaluated by ESI-MS

analysis. In accordance with the ESI-MS data, fluorescence microscopic analysis revealed that the Diacyl-EPA and Diacyl-OLA fluorescence was hardly detected at 150 h and thereafter (Fig. 2). Thus, we learned that although EPA and OLA could be incorporated into the PE and PG, they could not be tracked visually because the fluorescent NBD-moiety was hydrolyzed and lost. Therefore, the NBD-labeled diacyl phospholipids are not suitable for continual visualization of EPA-containing phospholipids *in vivo*.

Synthesis of fluorescent eicosapentaenyl-group-containing phospholipids -- For continual visualization of phospholipids *in vivo*, we synthesized NBD-containing hydrolysis-resistant PE derivatives to prevent the release of the hydrocarbon chain from the phospholipids. It is expected that replacement of the ester bond at the *sn*-2 position of phospholipids with an ether bond suppresses the hydrolytic release of the hydrocarbon chain from the glycerol backbone. Accordingly, we synthesized the following ether phospholipids to use in the *in vivo* imaging experiments: *N*-NBD-1-oleoyl-2-eicosapentaenyl-*sn*-glycero-3-phosphoethanolamine (Acylalkyl-EPA), *N*-NBD-1-oleoyl-2-oleyl-*sn*-glycero-3-phosphoethanolamine (Acylalkyl-OLA), *N*-NBD-1-oleyl-2-eicosapentaenyl-*sn*-glycero-3-phosphoethanolamine (Dialkyl-EPA), and *N*-NBD-1,2-dioleyl-*sn*-glycero-3-phosphoethanolamine (Dialkyl-OLA) (Fig. 1 and Supplemental Data for the synthesis).

Cellular uptake and remodeling of fluorescent eicosapentaenyl-group-containing phospholipids -- We tested whether these synthetic ether phospholipids are incorporated into the cell membrane of *S. livingstonensis* Ac10. The total lipids isolated from the cells grown in the presence of Acylalkyl-EPA, Acylalkyl-OLA, Dialkyl-EPA, or Dialkyl-OLA were analyzed by electrospray ionization-tandem mass spectrometry (Figs. 3 and 4). NBD-labeled phospholipids were found in the cell membrane when any of the synthetic ether phospholipids were used (Fig. 3). We also found that Acylalkyl-EPA and Acylalkyl-OLA were hydrolyzed at the *sn*-1, but not *sn*-2, position to yield *N*-NBD-2-eicosapentaenyl-*sn*-glycero-3-phosphoethanolamine (Lysoalkyl-EPA) and *N*-NBD-2-oleyl-*sn*-glycero-3-phosphoethanolamine (Lysoalkyl-OLA), respectively, during cultivation (Fig. 4, white bars). In addition to Lysoalkyl-EPA and Lysoalkyl-OLA, re-acylated NBD-labeled phospholipids containing two hydrocarbon chains were produced at 200 and 250 h (Fig. 4, black bars). The ratio of the total amount of the NBD-labeled phospholipids to the total amount of the unlabeled phospholipids in the cells grown in the presence of Acylalkyl-EPA for 250 h was 9.8 +/- 3.1%. The composition of the fatty acyl chains at the *sn*-1 position of the NBD-labeled phospholipids derived from Acylalkyl-EPA is shown in Table 1. These phospholipids, constituting 1%–5% of the total NBD-labeled phospholipids, were produced by the incorporation of a bacterial fatty acyl chain into the *sn*-1 position. In contrast to Acylalkyl-EPA and Acylalkyl-OLA, Dialkyl-EPA and Dialkyl-OLA were incorporated into the cell membrane without remodeling, because the ether bonds at the *sn*-1 and *sn*-2 positions are both resistant to hydrolysis (Fig. 4).

Distribution of NBD-labeled phospholipids in the IM and OM -- *S. livingstonensis* Ac10 is a Gram-negative bacterium, possessing both OM and IM. We measured the amount of NBD-labeled phospholipids distributed in these membranes by the dithionite quenching assay (see "Experimental Procedures" and "Supplemental Data" for details). To identify the membrane-specific location of the NBD-labeled phospholipids, we prepared the following three samples from cells grown at 6°C for 250 h: non-treated, lysozyme-treated, and lysozyme-and-Triton X-100-treated cells (Fig. S1A). By using these samples, NBD-labeled phospholipids located in the OM_{out}, in the OM_{in} and IM_{out}, and in the IM_{in} can be measured. Note that OM_{in} and IM_{out} cannot be distinguished by this assay.

We calculated the ratio of the NBD fluorescence at the OM_{out}, OM_{in}+IM_{out}, and IM_{in} in the cells grown in the presence of Acylalkyl-EPA, Acylalkyl-OLA, Dialkyl-EPA, or Dialkyl-OLA for 250 h (Fig. 5). For Dialkyl-EPA and Dialkyl-OLA, the NBD fluorescence was found at the OM_{out} and OM_{in}+IM_{out}, but almost no fluorescence was found at the IM_{in}. In contrast, about 25% of the fluorescence was found at IM_{in} when Acylalkyl-EPA or Acylalkyl-OLA was added to the cells.

In these experiments, a large part of the NBD fluorescence was quenched even when non-treated cells were used. This is not due to

quenching of NBD-derivatives in the culture medium because the cells were washed well before dithionite treatment. The results rather indicate that a large part of the NBD-labeled phospholipids was localized in OM_{out}. This uneven distribution between the different membrane surfaces is probably due to slow flip-flop of the lipids.

Fluorescence microscopic analysis of the eicosapentaenyl-group-containing phospholipids -- We cultivated *S. livingstonensis* Ac10 at 6°C in LB medium containing the NBD-labeled ether phospholipids (Acylalkyl-EPA, Acylalkyl-OLA, Dialkyl-EPA, and Dialkyl-OLA) for fluorescence microscopic analysis. These cells showed more intense fluorescence than those grown in the presence of Diacyl-EPA or Diacyl-OLA, except for the cells grown in the presence of Dialkyl-OLA for 250 h (Fig. 2). The disappearance of the fluorescence from the cells grown in the presence of Dialkyl-OLA is probably due to degradation of the NBD-labeled phospholipids or their elimination from the cells (Fig. 3). We found that the fluorescence was localized at the center of the cells when they were grown in the presence of Acylalkyl-EPA for 200 h or longer, whereas this localization was not observed in cells grown in the presence of the control Acylalkyl-OLA (Figs. 2 and 6). Fluorescence localization was not observed also in the Dialkyl-EPA and Dialkyl-OLA experiment (Fig. 2).

To further characterize the fluorescence localization, the cellular nucleoids were stained with Hoechst 33342 in cells grown with Acylalkyl-EPA or Acylalkyl-OLA for 250 h. Each of the 15 randomly chosen cells undergoing cell division was divided into seven equally sized sections, and the fluorescence intensities of NBD and Hoechst 33342 in each segment were measured (Fig. 6B). We found that the NBD-labeled ether phospholipids were localized at the nucleoid occlusion site at the center of the Acylalkyl-EPA-treated cells undergoing cell division. This localization was not observed when Acylalkyl-OLA was used. On the other hand, the same localization as well as cellular uptake and remodeling were observed when the *sn*-1 oleoyl group of Acylalkyl-EPA was replaced by palmitoleoyl group (data not shown). Thus, the fluorescence localization at the center of the cells was dependent on the eicosapentaenyl-group of the phospholipid. The localization we observed in these experiments is in accordance with the physiological importance of EPA-containing phospholipids in cell division.

Imaging of Lysoalkyl-EPA and its analog, N-NBD-1-methyl-2-eicosapentaenyl-sn-glycero-3-phosphoethanolamine (Methylalkyl-EPA), in cell membranes -- As shown in Figs. 2 and 6, we found that NBD-phospholipids are localized at the center of the cells when Acylalkyl-EPA was added to the cells. Under this condition, some of the Acylalkyl-EPA added to the cells was converted into Lysoalkyl-EPA, which was subsequently re-acylated to form phospholipids with two hydrocarbon chains (Fig. 4). Thus, the fluorescent phospholipids localized at the center of the cells could be the Acylalkyl-EPA added to the cells, the converted Lysoalkyl-EPA, or the re-acylated phospholipids. To distinguish between these and examine whether Lysoalkyl-EPA produced from Acylalkyl-EPA was localized at the center of the cells, we synthesized a Lysoalkyl-EPA analog, Methylalkyl-EPA, for *in vivo* imaging (Fig. 1 and Supplemental Data for the synthesis). Methylalkyl-EPA retains hydrophilicity of Lysoalkyl-EPA, which is considered important for the molecule to traverse through the periplasmic space to reach the IM. However, it is not susceptible to acylation at the *sn*-1 position unlike Lysoalkyl-EPA. We also synthesized Lysoalkyl-EPA as a control (Fig. 1 and Supplemental Data for the synthesis).

S. livingstonensis Ac10 was grown in the presence of Lysoalkyl-EPA or Methylalkyl-EPA, and the cellular phospholipids were analyzed by ESI-MS. The amounts of NBD-labeled phospholipids found incorporated into the cells were not significantly different between Lysoalkyl-EPA and Methylalkyl-EPA (Fig. 3). We also determined the amounts of NBD-labeled phospholipids distributed to the OM and IM by the dithionite quenching assay (Fig. 5). NBD-labeled phospholipids were found not only in the OM_{out} and OM_{in}+IM_{out}, but also in the IM_{in}, irrespective of whether Lysoalkyl-EPA or Methylalkyl-EPA was used. Thus, Methylalkyl-EPA mimics Lysoalkyl-EPA in these respects. On the other hand, Methylalkyl-EPA is different from Lysoalkyl-EPA in that Methylalkyl-EPA was not acylated at the *sn*-1 position, as expected (Fig. 4). In the case of Lysoalkyl-EPA, the *sn*-1 position was acylated, and the acyl chain composition at the *sn*-1 position was similar to that of the NBD-phospholipids derived from

Acylalkyl-EPA (Table 1). Fluorescence microscopic analysis revealed that the fluorescence localization at the center of the cells was observed when Lysoalkyl-EPA was added to the cells, whereas this localization was not observed when Methylalkyl-EPA was used (Fig. 6). This finding suggested that the localization at the center of the cells was dependent on the acylation of position *sn*-1.

Fluorescence microscopic analysis of the cells treated with dithionite to quench the NBD-fluorescence in the OM_{out} -- *S. livingstonensis* Ac10 was grown at 6°C for 250 h in the presence of Acylalkyl-EPA or Lysoalkyl-EPA, and the NBD fluorescence in the OM_{out} was quenched with sodium dithionite before fluorescence microscopic analysis as described in Experimental Procedures and Supplemental Data. The relative fluorescence intensity at the cell division site was increased by the dithionite treatment of both Acylalkyl-EPA-labeled and Lysoalkyl-EPA-labeled cells (Fig. 7).

DISCUSSION

Identity of the fluorescent phospholipid localized at the center of the cells during cell division -- We found that the NBD-labeled fluorescent phospholipids localized to the nucleoid occlusion site at the cell center during cell division when Acylalkyl-EPA was added to *S. livingstonensis* Ac10 (Figs. 2 and 6). This localization was eicosapentaenyl-group-dependent, because this localization was not observed when the cells were grown in the presence of Acylalkyl-OLA. Notably, when another phospholipid containing the eicosapentaenyl group was used, namely, Dialkyl-EPA, this localization was not observed (Fig. 2). This may be because of the difference in their subcellular distribution. The NBD-labeled phospholipids were detected in the IM_{in} when Acylalkyl-EPA was used, whereas the NBD-labeled phospholipids were not found in the IM_{in} with Dialkyl-EPA (Fig. 5). This was likely because the *sn*-1 position of Dialkyl-EPA was not hydrolyzed, rendering it less capable of migrating into the IM_{in}. Because OM_{in} and IM_{out} cannot be distinguished by the dithionite quenching assay, it is possible that the NBD-labeled phospholipids did not even reach the IM_{out} when Dialkyl-EPA was used. Thus, the data indicate that the NBD-labeled phospholipids that localize at the nucleoid occlusion site may come from the IM. This view is supported by the fluorescence microscopic analysis of the cells treated with dithionite. Dithionite treatment of the cells to quench the NBD fluorescence at the OM_{out} increased relative fluorescence intensities at the cell division site (Fig. 7).

When we used Diacyl-EPA, the cells were not labeled efficiently. This was probably due to the catalytic action of the OM phospholipase A (15, 26, 27); this enzyme likely catalyzed the cleavage of both ester-bonded hydrocarbon chains in Diacyl-EPA. Thus, the resulting fluorescent *N*-NBD-*sn*-glycero-3-phosphoethanolamine was likely released from the OM because of its high hydrophilicity and was not subsequently incorporated into any cellular membrane components, rendering it impossible for us to detect it by fluorescence methods.

Acylalkyl-EPA was converted into Lysoalkyl-EPA (Fig. 4, white bars) and then re-acylated to form NBD-labeled phospholipids with two hydrocarbon chains, one of which was the eicosapentaenyl group and the other was an acyl group produced by the bacterial cells (Fig. 4, black bars). Thus, the fluorescent phospholipids observed in our study that localized to the cell center could be Acylalkyl-EPA, Lysoalkyl-EPA, or re-acylated phospholipids. We found that the fluorescent phospholipids localized to the center of the cells when Lysoalkyl-EPA, but not Methylalkyl-EPA, was used (Fig. 6). Methylalkyl-EPA mimics Lysoalkyl-EPA in its distribution in the OM and IM but differs from Lysoalkyl-EPA in that it cannot be acylated at the *sn*-1 position. Thus, the results suggest that the fluorescence localization at nucleoid occlusion site was not due to Lysoalkyl-EPA itself but due to re-acylated phospholipids. In Gram-negative bacteria, 2-acylglycerolphosphoethanolamine acyltransferase, an enzyme that catalyzes the acylation of lysophospholipids at the *sn*-1 position, is localized to the IM (28, 29). Considering that the NBD-labeled phospholipids were found in the IM when Lysoalkyl-EPA was added to the cells (Fig. 5), acylation of Lysoalkyl-EPA at the *sn*-1 position may have been catalyzed by this enzyme once it reached the IM; this allowed it to travel to the nucleoid occlusion site in the center of the bacterial cells.

Dialkyl-EPA and Dialkyl-OLA did not reach the IM_{in} (Fig. 5), suggesting that

phospholipids containing two hydrocarbon chains cannot traverse through the periplasmic space unless at least one of their hydrocarbon chains was cleaved off. The acyl group at the *sn*-1 position of Acylalkyl-EPA and Acylalkyl-OLA was probably hydrolyzed before they traversed through the periplasm to reach the IM. OM-resident phospholipase A most likely catalyzed this reaction to produce Lysoalkyl-EPA and Lysoalkyl-OLA, respectively (15, 26, 27). We consider that Lysoalkyl-EPA, produced by hydrolysis of Acylalkyl-EPA, is re-acylated at its *sn*-1 position after reaching the IM, and the re-acylated NBD-labeled phospholipids are localized at the nucleoid occlusion site at the cell center during cell division.

Mechanisms and significance of membrane microdomain formation enriched in polyunsaturated hydrocarbon chain-containing phospholipids -- We found that phospholipids containing an eicosapentaenyl group are enriched at the site of cell division. This is in accordance with our finding that EPA-containing phospholipids play an important functional role in the cell division in *S. livingstonensis* Ac10 (13). Although the molecular mechanism for the formation of the membrane domain enriched in polyunsaturated hydrocarbon chain remains unknown, we consider the following two possibilities. First, the phospholipids containing the eicosapentaenyl group are enriched in a membrane region with a high curvature because of their physicochemical properties. We consider this possibility because the bending rigidity of bilayers rich in phospholipids with a polyunsaturated hydrocarbon chain is known to be low (30). The cellular membrane at the site of cell division has a high curvature, which may cause the enrichment of phospholipids with the eicosapentaenyl group in this region. A second possibility is that phospholipids containing an eicosapentaenyl group interact with proteins localized at the center of the cells during cell division. Considering that EPA-containing phospholipids promote cell division, there may be a direct or indirect interaction between these phospholipids and cell-division-related proteins at the cell center. These interactions may cause enrichment of the eicosapentaenyl-group-containing phospholipids at the site of cell division.

Polyunsaturated hydrocarbon chains have much greater diversity of energetically accessible conformational states than saturated hydrocarbon chains (31). This allows polyunsaturated hydrocarbon chains to solvate membrane proteins with rough surfaces with little energetic penalty. Thus, interaction with EPA-containing phospholipids may be beneficial for the stability and function of various membrane proteins, including those involved in cell division. The molecular interactions between EPA-containing phospholipids and membrane proteins involved in cell division are currently under investigation to better understand the role of EPA-containing phospholipids at the site of cell division. The occurrence of such membrane microdomains in other organisms and their specific physiological roles should also be examined in future studies. In the present study, the visualization of the membrane microdomain enriched in phospholipids with a polyunsaturated hydrocarbon chain was enabled by using a newly synthesized fluorescent probe with an uncleavable bond between the hydrocarbon chain and the glycerol backbone. This type of probe would be useful in examining whether membrane microdomains like the ones we observed in this study occur more generally among various organisms.

REFERENCES

1. Singer, S. J. and Nicolson, G. L. (1972) *Science* **175,** 720-731
2. Lingwood, D. and Simons, K. (2010) *Science* **327,** 46-50
3. Matsumoto, K., Kusaka, J., Nishibori, A., and Hara, H. (2006) *Mol. Microbiol.* **61,** 1110-1117
4. Renner, L. D. and Weibel, D. B. (2011) *Proc. Natl. Acad. Sci. U.S.A.* **108,** 6264-6269
5. Lopez, D. and Kolter, R. (2010) *Genes Dev.* **24,** 1893-1902
6. Wall, R., Ross, R. P., Fitzgerald, G. F., and Stanton, C. (2010) *Nutr. Rev.* **68,** 280-289
7. Watts, G. F. and Mori, T. A. (2011) *Curr. Opin. Lipidol.* **22,** 70-71
8. Sato, S. B., Sato, S., Kawamoto, J., and Kurihara, T. (2010) *Prostaglandins Leukot. Essent. Fatty Acids* **84,** 31-37
9. Schmitz, G. and Ecker, J. (2008) *Prog. Lipid Res.* **47,** 147-155

10. Feller, S. E. and Gawrisch, K. (2005) *Curr. Opin. Struct. Biol.* **15,** 416-422
11. Carrillo-Tripp, M. and Feller, S. E. (2005) *Biochemistry* **44,** 10164-10169
12. Grossfield, A., Feller, S. E., and Pitman, M. C. (2006) *Proc. Natl. Acad. Sci. U.S.A.* **103,** 4888-4893
13. Kawamoto, J., Kurihara, T., Yamamoto, K., Nagayasu, M., Tani, Y., Mihara, H., Hosokawa, M., Baba, T., Sato, S. B., and Esaki, N. (2009) *J. Bacteriol.* **191,** 632-640
14. Kawamoto, J., Sato, T., Nakasone, K., Kato, C., Mihara, H., Esaki, N., and Kurihara, T. (2011) *Environ. Microbiol.* **13,** 2293-2298
15. Sato, S., Kurihara, T., Kawamoto, J., Hosokawa, M., Sato, S. B., and Esaki, N. (2008) *Extremophiles* **12,** 753-761
16. Kawamoto, J., Kurihara, T., Kitagawa, M., Kato, I., and Esaki, N. (2007) *Extremophiles* **11,** 819-826
17. Miyake, R., Kawamoto, J., Wei, Y.-L., Kitagawa, M., Kato, I., Kurihara, T., and Esaki, N. (2007) *Appl. Environ. Microbiol.* **73,** 4849-4856
18. Reutelingsperger, C. P., Dumont, E., Thimister, P. W., van Genderen, H., Kenis, H., van de Eijnde, S., Heidendal, G., and Hofstra, L. (2002) *J. Immunol. Methods.* **265,** 123-132
19. Emoto, K. and Umeda, M. (2000) *J. Cell Biol.* **149,** 1215-1224
20. Jao, C. Y., Roth, M., Welti, R., and Salic, A. (2009) *Proc. Natl. Acad. Sci. U.S.A.* **106,** 15332-15337
21. Kuerschner, L., Ejsing, C. S., Ekroos, K., Shevchenko, A., Anderson, K. I., and Thiele, C. (2005) *Nat. Methods* **2,** 39-45
22. Neef, A. B. and Schultz, C. (2009) *Angew. Chem. Int. Ed. Engl.* **48,** 1498-1500
23. Yamaji, A., Sekizawa, Y., Emoto, K., Sakuraba, H., Inoue, K., Kobayashi, H., and Umeda, M. (1998) *J. Biol. Chem.* **273,** 5300-5306
24. Bligh, E. G. and Dyer, W. J. (1959) *Can. J. Biochem. Physiol.* **37,** 911-917
25. Shindou, H., Hishikawa, D., Harayama, T., Yuki, K., and Shimizu, T. (2009) *J. Lipid Res.* **50 Suppl,** S46-51
26. Malinverni, J. C. and Silhavy, T. J. (2009) *Proc. Natl. Acad. Sci. U.S.A.* **106,** 8009-8014
27. Dekker, N. (2000) *Mol. Microbiol.* **35,** 711-717
28. Harvat, E. M., Zhang, Y. M., Tran, C. V., Zhang, Z., Frank, M. W., Rock, C. O., and Saier, M. H. Jr. (2005) *J. Biol. Chem.* **280,** 12028-12034
29. Hsu, L., Jackowski, S., and Rock, C. O. (1991) *J. Biol. Chem.* **266,** 13783-13788
30. Rawicz, W., Olbrich, K. C., McIntosh, T., Needham, D., and Evans, E. (2000) *Biophys. J.* **79,** 328-339
31. Feller, S. E. (2008) *Chem. Phys. Lipids* **153,** 76-80

Acknowledgments -- We thank Prof. Masaaki Okazaki (Hirosaki University) for helpful advice on chemical synthesis.

FOOTNOTES

*This work was supported in part by the Grants-in-Aid for Scientific Research (B) from JSPS (20360372 and 22404021 to T.K.); Grant-in-Aid for Challenging Exploratory Research 22658028 (to T.K.); a Grant from the Institute for Fermentation, Osaka (to T.K.); a Grant from Japan Foundation for Applied Enzymology (to T.K.); a Grant for Research for Promoting Technological Seeds 10-041 from JST (to J.K.); and JSPS Research Fellowships for Young Scientists (to S.S.).

The abbreviations used are: EPA, eicosapentaenoic acid (20:5 $_{5,8,11,14,17\ \text{all cis}}$); DHA, docosahexaenoic acid (22:6 $_{4,7,10,13,16,19\ \text{all cis}}$); NBD, 7-nitro-2,1,3-benzoxadiazol-4-yl; PE, phosphatidylethanolamine; PG, phosphatidylglycerol; OLA, oleic acid; ESI-MS, electrospray ionization mass spectrometry; OM, outer membrane; IM, inner membrane; OM_{out}, outer leaflet of OM; OM_{in}, inner leaflet of OM; IM_{out}, outer leaflet of IM; IM_{in}, inner leaflet of IM.

FIGURE LEGENDS

FIGURE 1. NBD-labeled phospholipids synthesized in this study. Diacyl-EPA, Diacyl-OLA, Acylalkyl-EPA, Acylalkyl-OLA, Dialkyl-EPA, and Dialkyl-OLA were named after the binding mode between the glycerol moiety and the hydrocarbon chains, as well as the hydrocarbon chain species at the *sn*-2 position. Acylalkyl-EPA, Acylalkyl-OLA, Dialkyl-EPA, Dialkyl-OLA, Methylalkyl-EPA, and Lysoalkyl-EPA correspond to the compounds **34**, **33**, **14**, **21**, **38**, and **40**, respectively, in Scheme S1 in Supplemental Data.

FIGURE 2. Fluorescence microscopic images of *S. livingstonensis* Ac10 grown in the presence of NBD-labeled phospholipids (Diacyl-EPA, Diacyl-OLA, Acylalkyl-EPA, Acylalkyl-OLA, Dialkyl-EPA, and Dialkyl-OLA) for 150, 200, and 250 h.

FIGURE 3. The amount of NBD-labeled phospholipids incorporated into the cells of *S. livingstonensis* Ac10 grown in the presence of Acylalkyl-EPA, Acylalkyl-OLA, Dialkyl-EPA, Dialkyl-OLA, Lysoalkyl-EPA, and Methylalkyl-EPA for 50 (white), 100 (light gray), 150 (dark gray), and 200 h (black). The amount was calculated as described in Experimental Procedures and Supplemental Data. The mean ± S.D. of three separate measurements is shown.

FIGURE 4. Composition of NBD-labeled phospholipids in the cells of *S. livingstonensis* Ac10. The cells were grown in the presence of Acylalkyl-EPA, Acylalkyl-OLA, Dialkyl-EPA, Dialkyl-OLA, Lysoalkyl-EPA, and Methylalkyl-EPA for 100, 150, 200, and 250 h. Structures of NBD-labeled phospholipids extracted from the cells were analyzed by ESI-MS. The gray bars indicate externally added double-chain phospholipids. The white bars indicate single-chain phospholipids derived from Acylalkyl-EPA and Acylalkyl-OLA and externally added Lysoalkyl-EPA and Methylalkyl-EPA. The black bars indicate double-chain phospholipids produced in *S. livingstonensis* Ac10 by acylation of the *sn*-1 position of the single-chain phospholipids. The mean ± S.D. of three separate measurements is shown.

FIGURE 5. The distribution of NBD-labeled phospholipids in the OM_{out} (*white*), OM_{in} + IM_{out} (*gray*), and IM_{in} (*black*). The cells were grown in the presence of the various NBD-labeled phospholipids indicated. The mean ± S.D. of three separate determinations is shown.

FIGURE 6. Fluorescence microscopic images of *S. livingstonensis* Ac10 grown in the presence of NBD-labeled phospholipids. (*A*) Fluorescence microscopic images of the cells stained with Hoechst 33342 (false-colored red) (*left*) and NBD-labeled phospholipids (*center*) and merged images (*right*). The cells were grown at 6°C for 250 h in the presence of NBD-labeled phospholipids indicated at the left. The scale bars correspond to 5 μm. (*B*) Quantification of subcellular localization of NBD-labeled phospholipids and Hoechst 33342. The cells were grown in the presence of Acylalkyl-EPA (I), Acylalkyl-OLA (II), Lysoalkyl-EPA (III), and Methylalkyl-EPA (IV) at 6°C for 250 h. In each case, 15 cells during cell division were randomly chosen, and fluorescence intensities in seven equally sized sections of the cells (#1–#7) were determined by using ImageJ software. The closed symbols indicate the fluorescence of NBD-labeled phospholipids, and the open symbols indicate the fluorescence of Hoechst 33342.

FIGURE 7. Fluorescence microscopic images of dithionite-treated *S. livingstonensis* Ac10 grown in the presence of NBD-labeled phospholipids. (*A*) Fluorescence microscopic images of the cells stained with Hoechst 33342 (false-colored red) (*left*) and NBD-labeled phospholipids (*center*) and merged images (*right*). The cells were grown at 6°C for 250 h in the presence of Acylalkyl-EPA or Lysoalkyl-EPA as indicated at the left. For each of the Acylalkyl-EPA-labeled and Lysoalkyl-EPA-labeled cells, fluorescence images with (*upper*) or without (*lower*) treatment of dithionite are shown. The scale bars correspond to 5 μm. (*B*) Quantification of subcellular localization of NBD-labeled phospholipids and Hoechst 33342. The cells were grown in the presence of

Acylalkyl-EPA (I) and Lysoalkyl-EPA (II) at 6°C for 250 h. In each case, 15 cells during cell division were randomly chosen, and fluorescence intensities in seven equally sized sections of the cells (#1–#7) were determined by using ImageJ software. The closed symbols indicate the fluorescence of NBD-labeled phospholipids, and the open symbols indicate the fluorescence of Hoechst 33342. The dotted and solid lines indicate fluorescence intensities of the cells with and without treatment with dithionite, respectively.

Table 1. Composition of the *sn*-1 acyl chain of NBD-phospholipids from the cells cultivated with Acylalkyl-EPA and Lysoalkyl-EPA.

sn-1 acyl chain	Relative amount (%)	
	Acylalkyl-EPA	Lysoalkyl-EPA
13:0	4.0 ± 0.3	4.1 ± 0.6
13:1	1.2 ± 0.6	1.6 ± 0.6
14:0	4.0 ± 2.6	4.7 ± 2.6
14:1	1.6 ± 1.0	1.8 ± 1.0
15:0	19.0 ± 9.2	24.5 ± 12.3
15:1	0.9 ± 0.2	1.3 ± 0.6
16:0	0.7 ± 0.1	1.0 ± 0.2
16:1	29.6 ± 6.4	37.2 ± 11.4
17:0	6.6 ± 0.6	8.2 ± 0.7
17:1	3.3 ± 0.5	4.1 ± 0.2
18:0	2.1 ± 0.4	2.7 ± 0.6
18:1	27.0 ± 2.1	8.8 ± 1.1
20:5	N.D.	N.D.

Figure 1

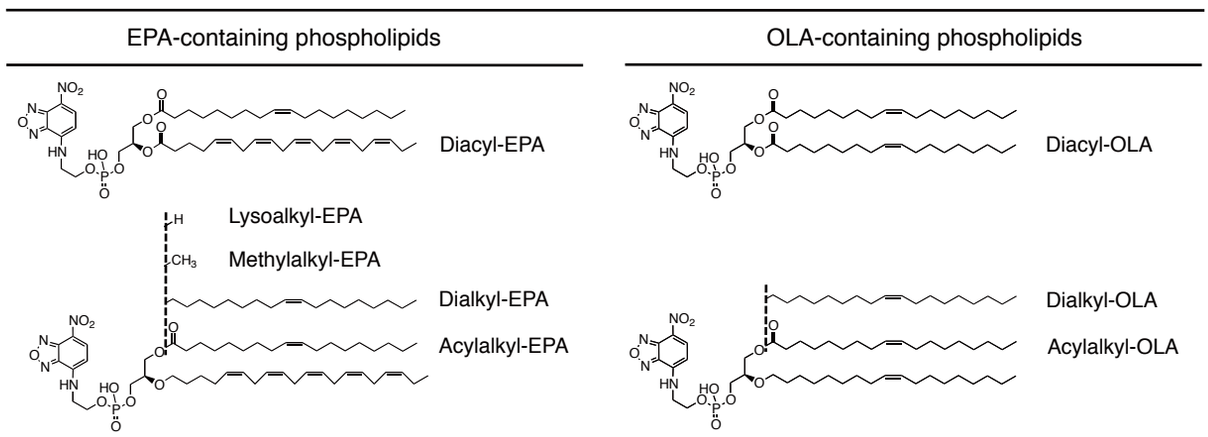
EPA-containing phospholipids
OLA-containing phospholipids
Diacyl-EPA
Diacyl-OLA
Lysoalkyl-EPA
Methylalkyl-EPA
Dialkyl-EPA
Acylalkyl-EPA
Dialkyl-OLA
Acylalkyl-OLA

Figure 2

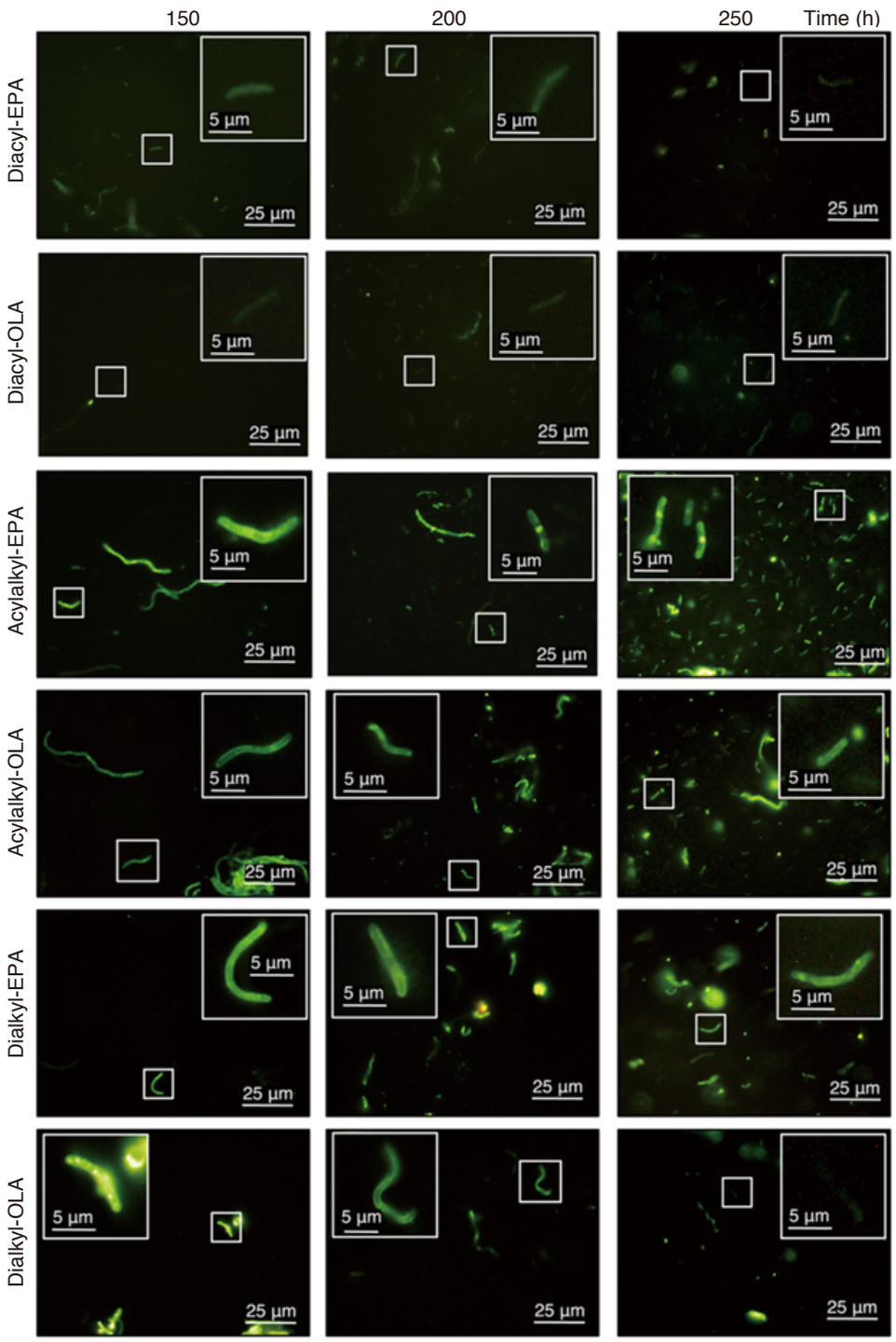
150
200
250
Time (h)
Diacyl-EPA
Diacyl-OLA
Acylalkyl-EPA
Acylalkyl-OLA
Dialkyl-EPA
Dialkyl-OLA
5 µm
25 µm

Figure 3

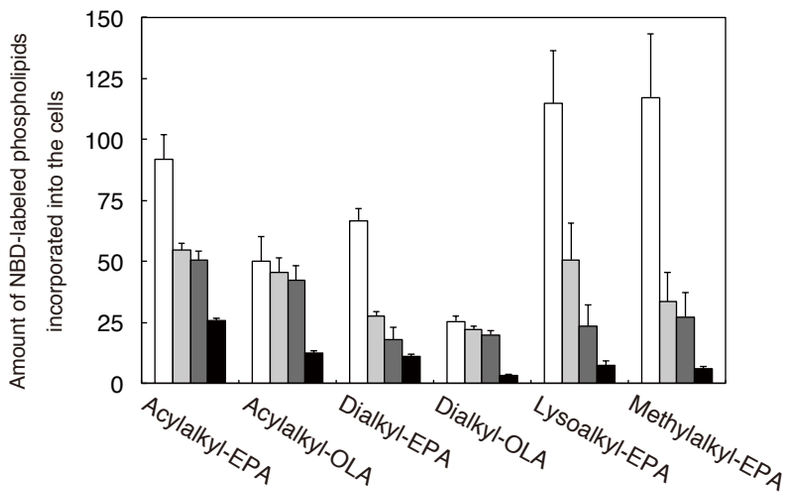
Amount of NBD-labeled phospholipids incorporated into the cells
150
125
100
75
50
25
0
Acylalkyl-EPA
Acylalkyl-OLA
Dialkyl-EPA
Dialkyl-OLA
Lysoalkyl-EPA
Methylalkyl-EPA

Figure 4

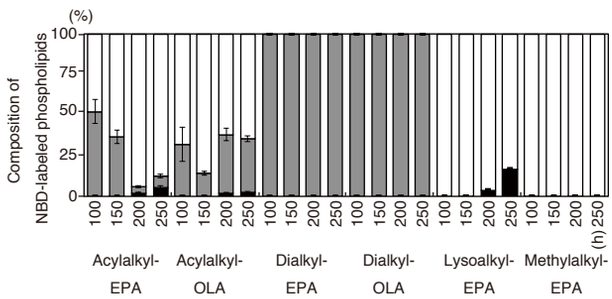
(%)
100
75
50
25
0
Composition of
NBD-labeled phospholipids
100 150 200 250 100 150 200 250 100 150 200 250 100 150 200 250 100 150 200 250 100 150 200 250 (h)
Acylalkyl-
EPA
Acylalkyl-
OLA
Dialkyl-
EPA
Dialkyl-
OLA
Lysoalkyl-
EPA
Methylalkyl-
EPA

Figure 5

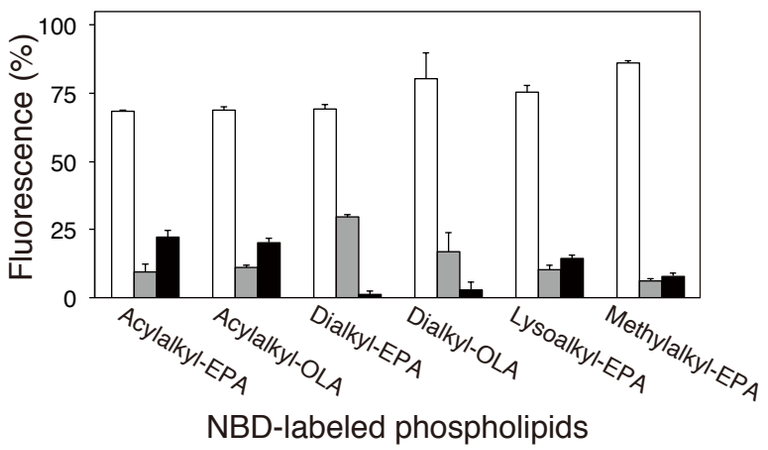
Fluorescence (%)
100
75
50
25
0
Acylalkyl-EPA
Acylalkyl-OLA
Dialkyl-EPA
Dialkyl-OLA
Lysoalkyl-EPA
Methylalkyl-EPA
NBD-labeled phospholipids

Figure 6

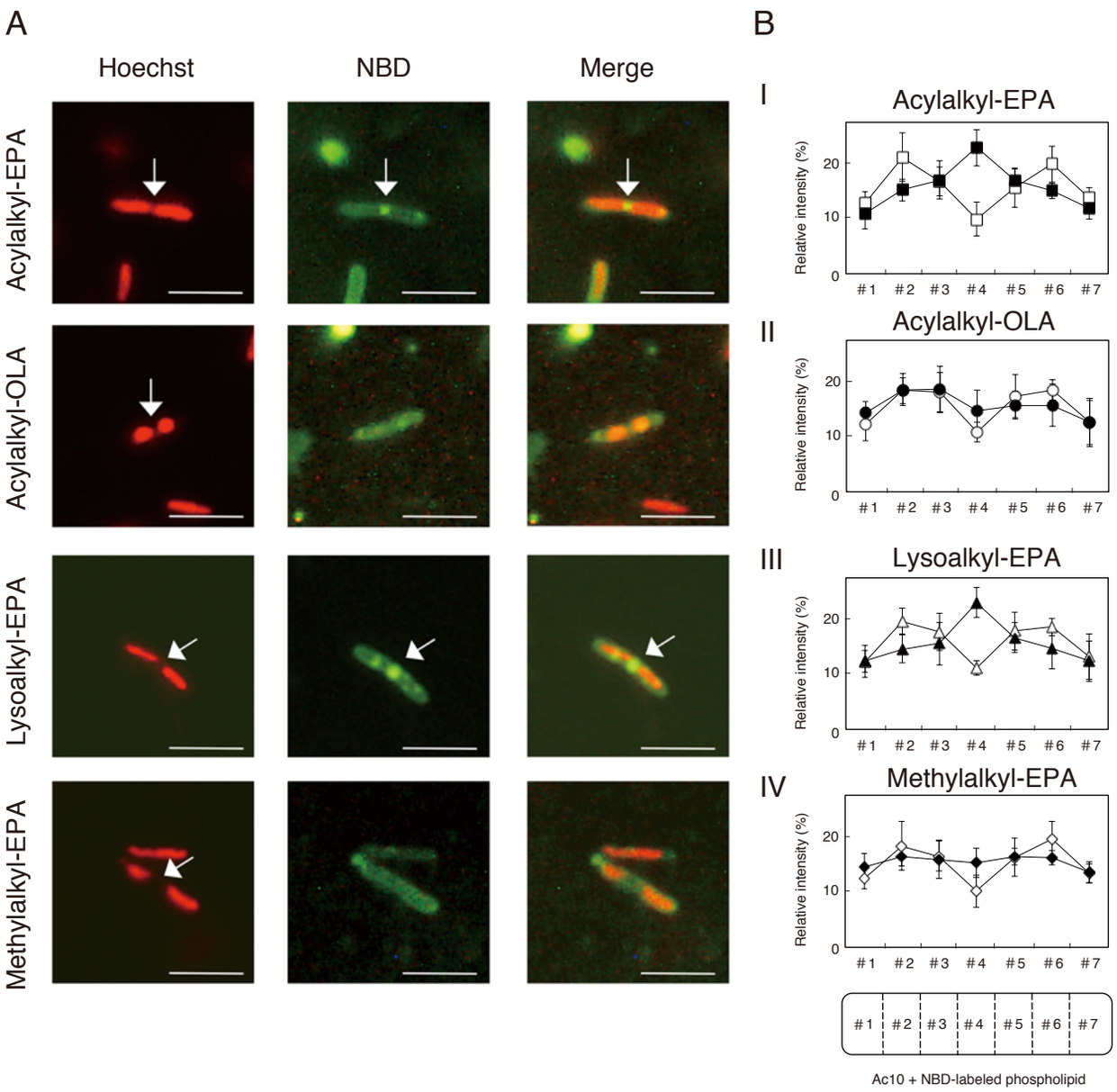
A
Hoechst
NBD
Merge
Acylalkyl-EPA
Acylalkyl-OLA
Lysoalkyl-EPA
Methylalkyl-EPA
B
I
Acylalkyl-EPA
II
Acylalkyl-OLA
III
Lysoalkyl-EPA
IV
Methylalkyl-EPA
Relative intensity (%)
0
10
20
#1 #2 #3 #4 #5 #6 #7
Ac10 + NBD-labeled phospholipid

Figure 7

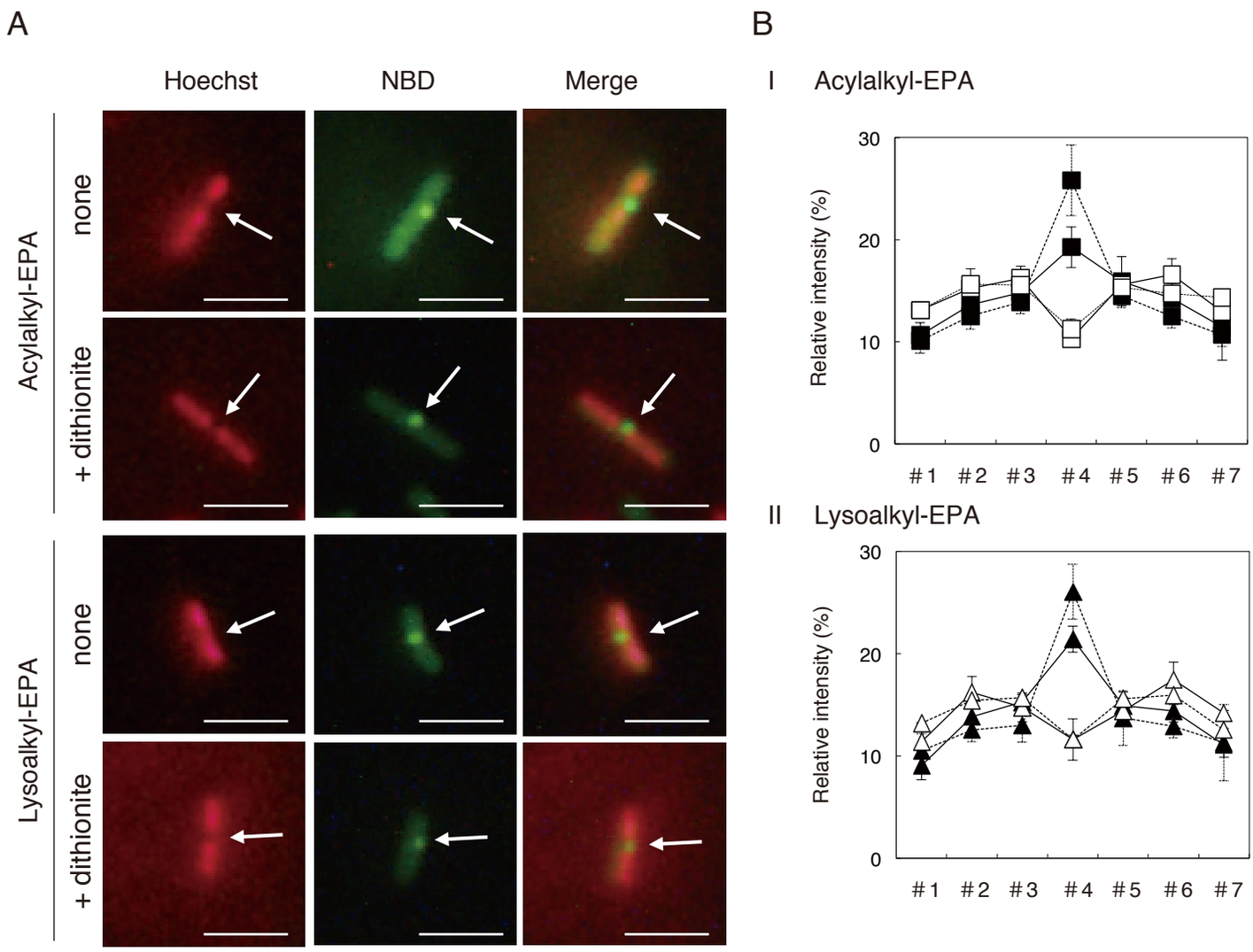
A
Hoechst
NBD
Merge
Acylalkyl-EPA
none
+ dithionite
Lysoalkyl-EPA
none
+ dithionite
B
I Acylalkyl-EPA
Relative intensity (%)
30
20
10
0
#1 #2 #3 #4 #5 #6 #7
II Lysoalkyl-EPA
Relative intensity (%)
30
20
10
0
#1 #2 #3 #4 #5 #6 #7

Supplemental Data

Occurrence of Bacterial Membrane Microdomain at the Cell Division Site Enriched in Phospholipids with Polyunsaturated Hydrocarbon Chain

Sho Sato, Jun Kawamoto, Satoshi B. Sato, Bunta Watanabe, Jun Hiratake, Nobuyoshi Esaki, and Tatsuo Kurihara

Supplementary Experimental Procedures

Synthesis of fluorescent probes

Unless otherwise specified, materials were obtained from commercial suppliers—Sigma-Aldrich Co., Tokyo Chemical Industry Co., Ltd., and Wako Pure Chemical Industries, Ltd.—at the highest level of purity available and were used without further purification. Dry solvents were purchased from Wako Pure Chemical Industries, Ltd., and used in the form supplied. Flash chromatography was carried out using silica gel 60N (spherical and neutral, particle diameter: 40–50 μm; Kanto Chemical Co., Inc.). Thin-layer chromatography (TLC) was performed on glass-backed precoated silica gel plates (Merck silica gel 60 F_{254} and 60). Spots were detected with a UV hand lamp at 254 nm or by staining with either iodine vapor or 0.65% (w/v) molybdate dissolved in H_2SO_4/H_2O (10:90 v/v). Synthesized compounds were characterized by NMR (^{1}H and, if appropriate, ^{31}P) and/or MS. NMR spectra were recorded using a Bruker UltraShield^{TM} Advance 400 (400 MHz, ^{1}H; 160 MHz, ^{31}P) spectrometer or JEOL JNM-AL-300 (300 MHz, ^{1}H) FT NMR system spectrometer. The instrument was calibrated using residual undeuterated solvent and tetramethylsilane as internal references. Mass spectra were recorded by electrospray ionization mass spectrometry

(ESI-MS) with an Applied Biosystems API3000 LC/MS/MS system.

Diacyl-EPA and Diacyl-OLA were synthesized by introducing the NBD group into phosphatidylethanolamine containing EPA (OEPE) and OLA (DOPE), respectively, by the same method described for compound **14**. OEPE and DOPE were synthesized as described previously (1). The synthetic route for other fluorescent probes used in this study is summarized in Scheme S1. The methods for the synthesis of individual compounds are described below.

Compound **3**

To a magnetically stirred mixture of oleic acid (**1**, 2.51 g, 8.90 mmol) in 40 ml dry tetrahydrofuran (THF) on ice was added $LiAlH_4$ (1.01 g, 26.7 mmol) by bits. The reaction mixture was stirred at room temperature for 1 h and then cooled on ice. Excess $LiAlH_4$ was quenched with 1 ml of water and 4 ml of 10% (w/v) aqueous NaOH solution, and the mixture was dried over magnesium sulfate. The mixture was then suction-filtered, and the filtrate was evaporated to afford the crude product (2.49 g) as a colorless oil, which was used for the subsequent synthesis without further purification. *Rf* = 0.15 (benzene). ^{1}H-NMR (300 MHz, $CDCl_3$): δ 5.42-5.28 (m, 2H), 3.64 (dt, 2H, *J* = 5.4 and 5.4), 2.12-1.96 (m, 4H), 1.57 (tt, 2H, *J* = 7.2 and 7.2), 1.43-1.19 (m, 22H), 0.89 (t, 3H, *J* = 6.9).

Compound **4**

Using a procedure similar to that described for the preparation of **3**, crude compound **4** (0.826 g) was obtained from EPA (0.765 g, 2.53 mmol). *Rf* = 0.15 (benzene). ^{1}H-NMR (300 MHz, $CDCl_3$): δ 5.62-5.27 (m, 10H), 3.65 (dt, *J* = 6.0 and 6.0, 2H), 2.92-2.74

(m, 8H), 2.18-2.02 (m, 4H), 1.62-1.52 (m, 2H), 1.51-1.39 (m, 2H), 0.98 (t, 3H, *J* = 7.4).

Compound **5**

Compound **3** (2.35 g, 8.75 mmol) and triethylamine (2.70 g, 26.7 mmol) were dissolved in 30 ml of dry benzene at room temperature under a nitrogen atmosphere. To this solution was added methanesulfonyl chloride (3.06 g, 26.7 mmol). After stirring for 2 h, the reaction mixture was suction-filtered, and subsequent removal of solvent of the filtrate under reduced pressure afforded a crude product, which was purified by flash column chromatography (eluted with hexane/ethyl acetate = 95:5 to 80:20) to yield compound **5** (2.45 g, 7.07 mmol) as a colorless oil. *Rf* = 0.35 (benzene). ^{1}H-NMR (300 MHz, $CDCl_3$): δ 5.45-5.30 (m, 2H), 4.22 (t, 2H, *J* = 6.0), 3.01 (s, 3H), 2.08-1.96 (m, 4H), 1.75 (tt, 2H, *J* = 6.8 and 6.8), 1.60-1.10 (m, 22H), 0.89 (t, 3H, *J* = 7.5).

Compound **6**

Using a procedure similar to that described for the preparation of **5**, compound **6** (1.13 g, 3.08 mmol, 93%) was obtained. *Rf* = 0.35 (benzene). ^{1}H-NMR (300 MHz, $CDCl_3$): δ 5.46-5.26 (m, 10H), 4.23 (t, 2H, *J* = 6.5), 3.00 (s, 3H), 2.88-2.75 (m, 8H), 2.16-2.03 (m, 4H), 1.83-1.70 (m, 2H), 1.54-1.44 (m, 2H), 0.98 (t, 3H, *J* = 7.4).

Compound **8**

To a magnetically stirred mixture of NaH (0.136 g, 3.41 mmol) in 5 ml dry DMSO at room temperature was added (*R*)-(2,2-dimethyl-1,3-dioxolan-4-yl)methanol (**7**, 0.300 g, 2.27 mmol) of dissolved in 5 ml dry DMSO dropwise. To the resulting solution, compound **5**

(0.866 g, 2.50 mmol) dissolved in 10 ml dry DMSO was slowly added, and the reaction mixture was stirred for 20 h. The reaction mixture was then poured into water (250 ml) and extracted with hexane (250 ml). The combined organic layers were concentrated under reduced pressure to obtain compound **8** (0.578 g, 1.51 mmol, 67%), which was used for the subsequent synthesis without further purification. *Rf* = 0.54 (hexane/ethyl acetate = 9:1). ^{1}H-NMR (300 MHz, $CDCl_3$): δ 5.40-5.28 (m, 2H), 4.26 (tt, 1H, *J* = 5.6 and 5.6), 4.06 (dd, 1H, *J* = 8.1 and 6.6), 3.73 (dd, 1H, *J* = 8.3 and 6.5), 3.54-3.37 (m, 4H), 2.06-1.94 (m, 4H), 1.60-1.56 (tt, 2H, *J* = 6.0 and 6.0), 1.42 (s, 3H), 1.36 (s, 3H), 1.24-1.34 (m, 22H), 0.82-0.85 (t, 3H, *J* = 7.2).

Compound **9**

Compound **8** (0.578 g, 1.51 mmol) was dissolved in dry $CHCl_3$ (15 ml) at room temperature under a nitrogen atmosphere. To the mixture was added 0.5 N HCl in 15 ml methanol. After stirring for 1 h, subsequent removal of the solvent under reduced pressure afforded **9** (0.535 g, 1.51 mmol, 100%), which was used for the subsequent synthesis without further purification. *Rf* = 0.07 (hexane/ethyl acetate = 3:2).

Compound **10**

Compound **9** (0.535 g, 1.51 mmol) and diisopropylethylamine (0.293 g, 2.27 mmol) were dissolved in 3.1 ml of dry dichloromethane at room temperature under a nitrogen atmosphere. To this solution was added triphenylmethyl chloride (0.462 g, 1.66 mmol). After stirring for 14 h, the reaction mixture was concentrated under reduced pressure to afford a crude product, which was purified by flash column chromatography (eluted with hexane/

ethyl acetate = 98:2 to 95:5) to yield compound **10** (0.861 g, 1.47 mmol, 97%) as a colorless oil. *Rf* = 0.31 (hexane/ethyl acetate = 9:1). ^{1}H-NMR (300 MHz, $CDCl_3$): δ 7.48-7.22 (m, 15H), 5.35-5.29 (m, 2H), 3.95-3.91 (m, 1H), 3.56-3.40 (m, 4H), 3.21 (dd, 1H, *J* = 9.3 and 5.7), 3.17 (dd, 1H, *J* = 9.3 and 5.4), 2.40 (d, 1H, *J* = 4.8), 2.04-1.98 (m, 4H), 1.59-1.49 (m, 2H), 1.39-1.32 (m, 22H), 0.88 (t, 3H, *J* = 6.9).

Compound **11**

Compound **10** (0.585 g, 1.00 mmol) and powdered KOH (0.272 g, 4.12 mmol) were dissolved in dry benzene (21 ml) at room temperature under a nitrogen atmosphere. Compound **6** (0.367 g, 1.00 mmol) dissolved in 6 ml dry benzene was slowly added to the resulting solution, and the reaction mixture was stirred for 2 h at 40˚C. The mixture was poured into water, and the product was extracted with hexane. After the solvent was removed under the reduced pressure, the crude product was purified by flash column chromatography (eluted with hexane/ethyl acetate = 99:1 to 98:2) to yield compound **11** (0.235 g, 0.275 mmol, 28%) as a colorless oil. *Rf* = 0.63 (hexane/ethyl acetate = 4:1). ^{1}H-NMR (300 MHz, $CDCl_3$): δ 7.48-7.22 (m, 15H), 5.42-5.29 (m, 12H), 3.60-3.35 (m, 7H), 3.25-3.15 (m, 2H), 2.87-2.75 (m, 8H), 2.12-1.95 (m, 8H), 1.65-1.40 (m, 6H), 1.39-1.21 (m, 22H), 0.97 (t, 3H, *J* = 7.7), 0.88 (t, 3H, *J* = 6.6).

Compound **12**

Compound **11** (0.334 g, 0.457 mmol) was dissolved in dry $CHCl_3$ (25 ml) at room temperature under a nitrogen atmosphere. To the mixture was added 0.5 N HCl in 25 ml methanol. After stirring for 1 h, subsequent removal of the solvent under reduced pressure

afforded the crude product, which was purified by flash column chromatography (eluted with hexane/ethyl acetate = 97:3 to 9:1) to yield compound **12** (0.176 g, 0.287 mmol, 63%) as a colorless oil. *Rf* = 0.26 (hexane/ethyl acetate = 4:1). ^{1}H-NMR (300 MHz, $CDCl_3$): δ 5.45-5.25 (m, 12H), 3.78-3.68 (m, 1H), 3.67-3.48 (m, 6H), 3.48-3.38 (t, 2H, *J* = 6.6), 2.85-2.75 (m, 8H), 2.18-1.90 (m, 8H), 1.63-1.56 (m, 4H), 1.43 (tt, 2H, *J* = 7.7 and 7.7), 1.32-1.26 (m, 22H), 0.98 (t, 3H, *J* = 7.7), 0.88 (t, 3H, *J* = 6.6).

Compound **13**

Phosphorous oxychloride (65.9 mg, 0.431 mmol) was dissolved in 0.45 ml of hexane and stirred at 5˚C. After the addition of triethylamine (43.5 mg, 0.431 mmol) dissolved in 0.9 ml of trichloroethylene, stirring was continued, and a solution of compound **12** (0.176 g, 0.287 mmol) in 3.5 ml of trichloroethylene was added dropwise over 30 min. After 1 h, the reaction mixture was filtered. Then 1 ml of toluene was added to the filtrate, and removed under the reduced pressure to afford the crude oil. To a magnetically stirred solution of the crude oil and triethylamine (116 mg, 1.15 mmol) in 4.3 ml of dry THF at 0˚C was added a solution of 2-aminoethanol (21.9 mg, 0.359 mmol) in 0.5 ml of dry THF. Then, the mixture was warmed to room temperature and kept stirring for 30 min. After an additional 30 min, the reaction mixture was suction-filtered. The filtrate solvent was removed under the reduced pressure to give the white crude oil. To a solution of the white crude oil in 5.7 ml of 2-propanol was added 2.9 ml of acetic acid/water (1:4), and then the reaction mixture was stirred magnetically for 2 h. The mixture was poured into 30 ml of chloroform/methanol/water (1:1:0.9), and the lower layer was collected and evaporated to afford the white solid, which was purified by flash column chromatography (eluted with

chloroform/methanol = 8:2 to 7:3) to yield compound **13** (0.187 g, 0.254 mmol, 89%) as a white solid. *Rf* = 0.44 (chloroform/methanol/28% NH_3 solution = 65:25:4). ^{1}H-NMR (400 MHz, $CDCl_3$): δ 8.68-8.42 (br s, 2H), 5.48-5.26 (m, 12H), 4.15-4.04 (br s, 2H), 3.91 (dd, 1H, *J* = 9.2 and 5.3), 3.87 (dd, 1H, *J* = 9.3 and 5.3), 3.63-3.35 (m, 7H), 3.23-3.05 (br s, 2H), 2.88-2.76 (m, 8H), 2.12-1.97 (m, 8H), 1.62-1.48 (m, 4H), 1.40 (m, 2H), 1.35-1.20 (m, 22H), 0.97 (t, 3H, *J* = 7.6), 0.88 (t, 3H, *J* = 7.0). ^{31}P-NMR (160 MHz, $CDCl_3$): δ 0.960. ESI-MS: 734.6 $[M-H]^-$ ($C_{43}H_{78}O_6PN$).

Compound **14**

Into a brown-colored flask was placed a chloroform solution (3.5 ml) of compound **13** (36.8 mg, 0.050 mmol), 4-fluoro-7-nitrobenzofurazan (NBD-F) (Dojindo Laboratories, Kumamoto, Japan) (30.2 mg, 0.165 mmol), and triethylamine (17.2 mg, 0.170 mmol) under a nitrogen atmosphere. The mixture was stirred at room temperature for 1 h and subsequent removal of solvent under reduced pressure afforded a crude product, which was purified by flash column chromatography (eluted with benzene/methanol = 9:1) to yield 36.9 mg of compound **14** (36.9 mg, 0.041 mmol, 82 %). *Rf* = 0.73 (chloroform/methanol/28 % NH_3 solution = 65:25:4). ESI-MS: 897.6 $[M-H]^-$. ($C_{49}H_{79}O_9PN_4$).

Compound **16**

To a stirred mixture of NaH (1.09 g, 25.2 mmol) in dry THF (38 ml) was added dropwise (*S*)-(2,2-dimethyl-1,3-dioxolan-4-yl)methanol (**15**, 2.50 g, 18.9 mmol) at 0°C. After it was stirred at room temperature for 30 min and then cooled on ice, *p*-methoxybenzyl chloride (2.96 g, 18.9 mmol) was slowly added to the resulting solution. After refluxing at

70˚C overnight, the solvent was removed under reduced pressure. The residue was redissolved in hexane and suction-filtered. To the filtrate washed with the same volume of water twice was added magnesium sulfate followed by the second suction-filtration. Subsequent removal of the solvent under reduced pressure afforded the crude product **16**, which was used for the subsequent synthesis without further purification. *Rf* = 0.41 (hexane/ethyl acetate = 4:1). ^{1}H-NMR (300 MHz, $CDCl_3$): δ 7.26 (d, 2H, *J* = 8.4), 6.88 (d, 2H, *J* = 8.4), 4.52 and 4.49 (d, 1H, *J* = 9.9), 4.28 (tt, 1H, *J* = 6.3 and 6.3), 4.04 and 3.72 (dd, 1H, *J* = 8.3 and 6.3), 3.80 (s, 3H), 3.53 and 3.44 (dd, 1H, *J* = 9.7 and 5.4), 1.42 and 1.36 (s, 3H).

Compound **17**

To a magnetically stirred mixture of **16** (5.79 g, 22.9 mmol) dissolved in dry THF (45 ml) on ice was added dropwise 1 N HCl aqueous solution (45 ml). After stirring at room temperature for 10 h, 5 N NaOH aqueous solution was gently added to adjust to pH 8 on ice. The mixture was poured into saturated NaCl aqueous solution, and the product was extracted with ethyl acetate. After the solvent was removed under the reduced pressure, the crude product was purified by flash column chromatography (eluted with chloroform/methanol = 90:10 to 85:15) to yield compound **17** (4.52 g, 21.3 mmol, 93%) as a colorless oil. *Rf* = 0.13 (hexane/ethyl acetate = 3:2). ^{1}H-NMR (300 MHz, $CDCl_3$): δ 7.25 (d, 2H, *J* = 7.8), 6.89 (d, 2H, *J* = 8.7), 4.48 (s, 2H), 3.86 (tt, 1H, *J* = 5.0 and 5.0), 3.81 (s, 3H), 3.73-3.48 (m, 4H), 2.67 (d, 1H, *J* = 5.1), 2.20 (dd, 1H, *J* = 6.6 and 5.7).

Compound **18**

Compound **17** (0.213 g, 1.00 mmol), NaH (0.159 g, 4.00 mmol), and dry DMSO

(15 ml) were placed in a round-bottomed flask under a nitrogen atmosphere. Compound **5** (0.693 g, 2.00 mmol) dissolved in 2 ml of dry DMSO was then added, and the reaction mixture was stirred at room temperature for 24 h. To the reaction mixture was added water. The mixture was then extracted with ethyl acetate. After the combined organic layers were concentrated under reduced pressure, the crude product was purified by flash column chromatography (eluted with hexane/ethyl acetate = 97:3 to 95:5) to give compound **18** (0.320 g, 0.449 mmol, 45%) as a colorless oil. *Rf* = 0.33 (benzene). ^{1}H-NMR (300 MHz, $CDCl_3$): δ 7.25 (d, 2H, *J* = 8.7), 6.87 (d, 2H, *J* = 8.7), 5.40-5.29 (m, 4H), 4.48 (s, 2H), 3.80 (s, 3H), 3.60-3.36 (m, 9H), 2.04-1.98 (m, 8H), 1.60-1.47 (m, 4H), 1.40-1.20 (m, 44H), 0.88 (t, 6H, *J* = 6.6).

Compound **19**

Compound **18** (71.3 mg, 0.100 mmol) was dissolved in a mixture of 10 ml of dichloromethane and 133 μl of 0.1-M phosphate buffer solution (pH 7.2), and the resulting solution was stirred at 0˚C for 1 h. To the resulting solution was added of 2,3-dichloro-5,6-dicyano-*p*-benzoquinone (DDQ, 45.4 mg, 0.200 mmol), followed by additional stirring at room temperature for 2 h. The mixture was extracted with ethyl acetate. The solvent of the combined organic layers was then removed under reduced pressure. The resulting crude product was purified by flash column chromatography (hexane/ethyl acetate = 95:5), yielding compound **19** (45.2 mg, 76.1 μmol, 76%) as a colorless oil. *Rf* = 0.52 (hexane/ethyl acetate = 4:1). ^{1}H-NMR (300 MHz, $CDCl_3$): δ 5.40-5.30 (m, 4H), 3.77-3.67 (m, 1H), 3.66-3.35 (m, 8H), 2.01 (dd, 8H, *J* = 5.4 and 5.4), 1.62-1.52 (m, 4H), 1.40-1.20 (m, 44H), 0.88 (t, 6H, *J* = 6.6).

Compound **20**

Using a procedure similar to that described for the preparation of **13**, compound **20** (23.1 mg, 32.3 μmol, 19%) was obtained. *Rf* = 0.44 (chloroform/methanol/28% NH_3 solution = 65:25:4). ^{1}H-NMR (400 MHz, $CDCl_3$): δ 8.68-8.42 (br s, 2H), 5.48-5.26 (m, 4H), 4.15-4.04 (br s, 2H), 3.91 (dd, 1H, *J* = 9.2 and 5.3), 3.87 (dd, 1H, *J* = 9.3 and 5.3), 3.63-3.35 (m, 7H), 3.23-3.05 (br s, 2H), 2.12-1.97 (m, 8H), 1.62-1.48 (m, 4H), 1.35-1.20 (m, 44H), 0.88 (t, 6H, *J* = 7.0). ^{31}P-NMR (160 MHz, $CDCl_3$): δ 0.961. ESI-MS: 714.6 $[M-H]^-$ ($C_{41}H_{82}O_6PN$).

Compound **21**

Using a procedure similar to that described for the preparation of **14**, compound **21** (6.1 mg, 6.94 μmol, 69%) was obtained. *Rf* = 0.35 (benzene). *Rf* = 0.44 (chloroform/methanol/28% NH_3 solution (65/25/4, v/v/v)). ESI-MS: 877.6 $[M-H]^-$ ($C_{47}H_{83}O_9PN_4$).

Compound **22**

Compound **17** (1.26 g, 5.95 mmol) and diisopropylethylamine (1.15 g, 8.93 mmol) were dissolved in 13 ml of dry dichloromethane at room temperature under nitrogen atmosphere. To this solution was added triphenylmethyl chloride (1.83 g, 6.54 mmol). After stirring overnight, the reaction mixture was concentrated under reduced pressure. The residue was redissolved in benzene and purified by flash column chromatography (eluted with benzene/methanol = 98:2 to 9:1) to yield compound **22** (2.61 g, 5.72 mmol, 96%). *Rf* = 0.23 (hexane/ethyl acetate = 4:1). ^{1}H-NMR (300 MHz, $CDCl_3$): δ 7.45-7.18 (m, 17H), 6.86 (d, 2H,

J = 8.4), 4.46 (s, 2H), 3.96 (tt, 1H, *J* = 5.3 and 5.3), 3.80 (s, 3H), 3.57 (dd, 1H, *J* = 9.5 and 4.3), 3.52 (dd, 1H, *J* = 9.5 and 6.6), 3.22 (dd, 1H, *J* = 9.0 and 5.7), 3.18 (dd, 1H, *J* = 8.9 and 5.0), 2.39 (d, 1H, *J* = 4.8).

Compound **23**

Compound **22** (1.36 g, 3.00 mmol), NaH (0.263 g, 6.57 mmol), and dry DMSO (22 ml) were placed in a round-bottomed flask under a nitrogen atmosphere. Compound **5** (0.520 g, 1.5 mmol) dissolved in 3 ml of dry DMSO was then added, and the reaction mixture was stirred at room temperature for 5 h. To the reaction mixture was added water. The mixture was then extracted with hexane. After the combined organic layers were concentrated under reduced pressure, the crude product was purified by flash column chromatography (eluted with hexane/ethyl acetate = 98:2 to 9:1) to give compound **23** (0.688 g, 0.977 mmol, 65%) as a colorless oil. *Rf* = 0.56 (benzene). ^{1}H-NMR (300 MHz, $CDCl_3$): δ 7.47-7.41 (m, 6H), 7.32-7.15 (m, 11H), 6.83 (d, 2H, *J* = 8.7), 5.41-5.27 (m, 2H), 4.46 and 4.42 (d, 1H, *J* = 12.0), 2.93 (s, 3H), 3.62-3.47 (m, 5H), 3.19 (d, 2H, *J* = 4.2), 2.00 (m, 4H), 1.56 (tt, 2H, *J* = 6.9 and 6.9), 1.38-1.20 (m, 22H), 0.88 (t, 3H, *J* = 6.6).

Compound **24**

Compound **22** (0.326 g, 0.718 mmol) and powdered KOH (0.201 g, 3.05 mmol) were dissolved in dry benzene (15 ml) at room temperature under a nitrogen atmosphere. Compound **6** (0.263 g, 0.718 mmol) dissolved in 2 ml dry benzene was slowly added to the resulting solution, and the reaction mixture was stirred for 12 h at 40˚C. The mixture was poured into water, and the product was extracted with hexane. After the solvent was removed

in vacuo, the crude product was purified by flash column chromatography (eluted with hexane/ethyl acetate = 97:3 to 95:5) to yield compound **24** (0.216 g, 0.303 mmol, 42%) as a colorless oil. *Rf* = 0.63 (hexane/ethyl acetate = 4:1). ^{1}H-NMR (300 MHz, $CDCl_3$): δ 7.36-7.18 (m, 6H), 7.17-7.07 (m, 11H), 6.83 (d, 2H, *J* = 8.4), 5.44-5.29 (m, 10H), 4.45 and 4.42 (d, 1H, *J* = 12.0), 3.79 (s, 3H), 3.63-3.50 (m, 5H), 3.19 (d, 2H, *J* = 3.9), 2.88-2.78 (m, 8H), 2.14-2.02 (m, 4H), 1.64-1.55 (m, 2H), 1.43 (tt, 2H, *J* = 7.1 and 7.1), 0.97 (t, 3H, *J* = 7.5).

Compound **25**

Compound **23** (0.678 g, 0.961 mmol) was dissolved in dry $CHCl_3$ (75 ml) at room temperature under a nitrogen atmosphere. To the mixture was added 0.5 N HCl in 75 ml methanol. After stirring for 1 h, subsequent removal of the solvent under reduced pressure afforded the crude product, which was purified by flash column chromatography (eluted with hexane/ethyl acetate = 9:1 to 8:2) to yield compound **25** (0.317 g, 0.703 mmol, 73%) as a colorless oil. *Rf* = 0.26 (hexane/ethyl acetate = 4:1). ^{1}H-NMR (300 MHz, $CDCl_3$): δ 7.25 (d, 2H, *J* = 8.1), 6.88 (d, 2H, *J* = 8.4), 5.40-5.29 (m, 2H), 4.47 (s, 2H), 3.80 (s, 3H), 3.75-3.46 (m, 7H), 2.13-1.95 (m, 4H), 1.63-1.51 (m, 2H), 1.45-1.20 (m, 22H), 0.88 (t, 3H, *J* = 6.6).

Compound **26**

Using a procedure similar to that described for the preparation of **25**, compound **26** (137 mg, 0.291 mmol, 91%) was obtained. *Rf* = 0.26 (hexane/ethyl acetate = 4:1). ^{1}H-NMR (300 MHz, $CDCl_3$): δ 7.25 (d, 2H, *J* = 8.4), 6.88 (d, 2H, *J* = 8.7), 5.48-5.25 (m, 10H), 4.47 (s, 2H), 3.80 (s, 3H), 3.75-3.46 (m, 7H), 2.92-2.76 (m, 8H), 2.16-2.00 (m, 4H), 1.66-1.50 (m, 2H), 1.42 (tt, 2H, *J* = 7.5 and 7.5), 0.97 (t, 3H, *J* = 7.5).

Compound **27**

To a magnetically stirred mixture of **25** (105 mg, 0.228 mmol), dicyclohexylcarbodiimide (127 mg, 0.616 mmol), and dimethylaminopyridine (40.1 mg, 0.296 mmol) dissolved in 4.5 ml of dry chloroform was added oleic acid (142 mg, 0.502 mmol) under a nitrogen atmosphere at 0˚C. Subsequent removal of the solvent under reduced pressure after stirring for 11 h at room temperature afforded the crude product, which was purified by flash column chromatography (eluted with a mixture of hexane and ethyl acetate (98/2 to 95/5, v/v)) to yield compound **27** (156 mg, 0.220 mmol, 94%) as a colorless oil. *Rf* = 0.70 (hexane/ethyl acetate = 4:1). ^{1}H-NMR (300 MHz, $CDCl_3$): δ 7.25 (d, 2H, *J* = 8.7), 6.87 (d, 2H, *J* = 8.4), 5.41-5.26 (m, 4H), 4.48 (s, 2H), 4.23 (dd, 1H, *J* = 11.7 and 4.2), 4.11 (dd, 1H, *J* = 11.7 and 5.7), 3.80 (s, 3H), 3.64 (tt, 1H, *J* = 5.4 and 5.4), 3.58-3.46 (m, 4H), 2.29 (t, 2H, *J* = 7.5), 2.08-1.94 (m, 8H), 1.68-1.48 (m, 4H), 1.39-1.22 (m, 42H), 0.88 (t, 6H, *J* = 6.6).

Compound **28**

Using a procedure similar to that described for the preparation of **27**, compound **28** (143 mg, 0.192 mmol, 95%) was obtained. *Rf* = 0.53 (hexane/ethyl acetate = 4:1). ^{1}H-NMR (300 MHz, $CDCl_3$): δ 7.25 (d, 2H, *J* = 8.7), 6.87 (d, 2H, *J* = 8.4), 5.46-5.28 (m, 12H), 4.47 (s, 2H), 4.23 (dd, 1H, *J* = 11.6 and 4.4), 4.11 (dd, 1H, *J* = 11.4 and 5.7), 3.80 (s, 3H), 3.64 (tt, 1H, *J* = 5.0 and 5.0), 3.58-3.47 (m, 4H), 2.90-2.76 (m, 8H), 2.29 (t, 2H, *J* = 7.5), 2.14-1.96 (m, 8H), 1.68-1.52 (m, 4H), 1.41 (m, 2H), 1.36-1.24 (m, 20H), 0.97 (t, 3H, *J* = 7.5), 0.88 (t, 3H, *J* = 6.6).

Compound **29**

Using a procedure similar to that described for the preparation of **19**, compound **29** (136.5 mg, 0.226 mmol, 56%) was obtained. *Rf* = 0.37 (hexane/ethyl acetate = 4:1). ^{1}H-NMR (300 MHz, $CDCl_3$): δ 5.44-5.28 (m, 4H), 4.26-4.12 (m, 2H), 3.74-3.46 (m, 5H), 2.32 (t, 2H, *J* = 7.5), 2.08-1.94 (m, 8H), 1.72-1.52 (m, 4H), 1.42-1.22 (m, 42H), 0.88 (t, 6H, *J* = 6.6).

Compound **30**

Using a procedure similar to that described for the preparation of **19**, compound **30** (60.0 mg, 95.7 μmol, 48%) was obtained. *Rf* = 0.33 (hexane/ethyl acetate = 4:1). ^{1}H-NMR (300 MHz, $CDCl_3$): δ 5.38-5.21 (m, 12H), 4.10 (dd, 2H, *J* = 4.2 and 2.4), 3.65-3.41 (m, 5H), 2.78 (t, 4H, *J* = 4.8), 2.75 (t, 4H, *J* = 5.4), 2.29 (t, 2H, *J* = 7.5), 2.14-1.88 (m, 8H), 1.62-1.46 (m, 4H), 1.36 (m, 2H), 1.36-1.10 (m, 20H), 0.91 (t, 3H, *J* = 7.5), 0.81 (t, 3H, *J* = 6.6).

Compound **31**

Using a procedure similar to that described for the preparation of **13**, compound **31** (60.0 mg, 0.124 mmol, 75%) was obtained. *Rf* = 0.44 (chloroform/methanol/28% NH_3 solution = 65:25:4). ^{1}H-NMR (400 MHz, $CDCl_3$): δ 8.68-8.42 (br s, 2H), 5.45-5.28 (m, 4H), 4.28 (dd, 2H, *J* = 8.9 and 2.6), 4.15-4.04 (br s, 2H), 3.96-3.81 (br s, 2H), 3.64-3.48 (m, 3H), 3.19-3.12 (br s, 2H), 2.30 (t, 2H, *J* = 5.7), 2.12-1.97 (m, 8H), 1.62-1.50 (m, 4H), 1.36-1.20 (m, 42H), 0.88 (t, 6H, *J* = 5.3). ^{31}P-NMR (160 MHz, $CDCl_3$): δ 0.998.

Compound **32**

Using a procedure similar to that described for the preparation of **13**, compound **32**

(22.0 mg, 29.3 μmol, 30%) was obtained. *Rf* = 0.44 (chloroform/methanol/28% NH_3 solution = 65:25:4). ^{1}H-NMR (400 MHz, $CDCl_3$): δ 8.68-8.42 (br s, 2H), 5.48-5.25 (m, 12H), 4.28 (dd, 2H, *J* = 8.9 and 2.6), 4.15-4.04 (br s, 2H), 3.96-3.81 (br s, 2H), 3.64-3.48 (m, 3H), 3.19-3.12 (br s, 2H), 2.88-2.76 (m, 8H), 2.30 (t, 2H, *J* = 5.7), 2.12-1.97 (m, 8H), 1.62-1.50 (m, 4H), 1.40 (m, 2H), 1.36-1.20 (m, 20H), 0.97 (t, 3H, *J* = 5.7), 0.88 (t, 3H, *J* = 5.3). ^{31}P-NMR (160 MHz, $CDCl_3$): δ 1.051. ESI-MS: 748.6 $[M-H]^-$ ($C_{43}H_{76}O_7PN$).

Compound **33**

Using a procedure similar to that described for the preparation of **14**, compound **33** (17.3 mg, 19.4 μmol, 78%) was obtained. *Rf* = 0.35 (benzene). *Rf* = 0.67 (chloroform/methanol/28% NH_3 solution (65/25/4, v/v/v)). ESI-MS: 891.6 $[M-H]^-$ ($C_{47}H_{81}O_{10}PN_4$).

Compound **34**

Using a procedure similar to that described for the preparation of **14**, compound **34** (4.66 mg, 5.10 μmol, 92%) was obtained. *Rf* = 0.35 (benzene). *Rf* = 0.67 (chloroform/methanol/28% NH_3 solution = 65:25:4). ESI-MS: 911.4 $[M-H]^-$ ($C_{49}H_{77}O_{10}PN_4$)

Compound **35**

To a stirred mixture of NaH (50.0 mg, 1.25 mmol) in dry THF (16 ml) was added dropwise compound **26** (60.3 mg, 0.125 mmol) at 0˚C. After it was stirred at room temperature for 30 min and then cooled on ice, iodomethane (285 mg, 2.01 mmol) was slowly added to the resulting solution. To the reaction mixture was added water after stirring at 8˚C

for 16 h. The mixture was then extracted with ethyl acetate. After the combined organic layers were concentrated under reduced pressure, the crude product was purified by flash column chromatography (eluted with hexane/ethyl acetate = 90:10 to 80:20) to give compound **35** (59.7 mg, 0.120 mmol, 94%) as a colorless oil. *Rf* = 0.49 (hexane/ethyl acetate = 4:1). ^{1}H-NMR (300 MHz, $CDCl_3$): δ 7.25 (d, 2H, *J* = 8.4), 6.87 (d, 2H, *J* = 8.7), 5.44-5.27 (m, 10H), 4.48 (s, 2H), 3.80 (s, 3H), 3.61-3.41 (m, 7H), 3.35 (s, 3H), 2.88-2.77 (m, 8H), 2.14-2.01 (m, 4H), 1.60 (tt, 2H, *J* = 7.4 and 7.4), 1.42 (tt, 2H, *J* = 7.7 and 7.7), 0.97 (t, 3H, *J* = 7.5).

Compound **36**

Using a procedure similar to that described for the preparation of **19**, crude **36** was obtained, which was purified by flash column chromatography (hexane/ethyl acetate = 80:20), yielding compound **36** (8.0 mg, 21.2 μmol, 18%) as a colorless oil. *Rf* = 0.12 (hexane/ethyl acetate = 4:1). ^{1}H-NMR (300 MHz, $CDCl_3$): δ 5.44-5.27 (m, 10H), 3.75-3.43 (m, 7H), 3.37 (s, 3H), 2.88-2.77 (m, 8H), 2.14-2.01 (m, 4H), 1.60 (tt, 2H, *J* = 7.2 and 7.2), 1.43 (tt, 2H, *J* = 7.8 and 7.8), 0.97 (t, 3H, *J* = 7.5).

Compound **37**

Using a procedure similar to that described for the preparation of **13**, compound **37** (4.5 mg, 9.0 μmol, 41%) was obtained. *Rf* = 0.23 (chloroform/methanol/28% NH_3 solution = 65:25:4). ^{1}H-NMR (400 MHz, $CDCl_3$): δ 8.68-8.42 (br s, 2H), 5.48-5.26 (m, 10H), 4.15-4.04 (br s, 2H), 3.91 and 3.87 (dd, 1H, *J* = 9.3 and 5.3), 3.63-3.38 (m, 5H), 3.37 (s, 3H), 3.23-3.05 (br s, 2H), 2.88-2.76 (m, 8H), 2.12-2.02 (m, 4H), 1.60 (tt, 2H, *J* = 7.2 and 7.2), 1.43 (tt, 2H, *J* = 7.8 and 7.8), 0.97 (t, 3H, *J* = 7.5). ^{31}P-NMR (160 MHz, $CDCl_3$): δ 0.955. ESI-MS: 498.6

$[M-H]^-$ ($C_{26}H_{46}O_6PN$).

Compound **38**

Using a procedure similar to that described for the preparation of **14**, compound **38** (4.7 mg, 7.1 μmol, 80%) was obtained. *Rf* = 0.59 (chloroform/methanol/28% NH_3 solution = 65:25:4). ESI-MS: 661.6 $[M-H]^-$ ($C_{32}H_{47}O_9PN_4$).

Compound **39**

In a round bottom flask, an heterogenous mixture of compound **32** (5.0 mg, 6.6 μmol) dissolved in 0.13 ml of diisopropyl ether and phospholipase A_1 solution (0.65 ml of 50 mM sodium acetate (pH 4) containing 1.6 μl of Lecitase Ultra (phospholipase A_1 from *Thermomyces lanuginosus/Fusarium oxysporum*, Novozymes Co. Ltd)) was sonicated at 35 kHz under a nitrogen atmosphere at 35°C for 30 min by using an ultrasonic washer (SHARP, UT-105S). To the mixture after the reaction was added 1.6 ml of methanol. Then, 3.2 ml of hexane/diisopropyl ether (1:1) was added to the mixture followed by removal of the upper layer to separate compound **39** and free oleic acid. This wash was repeated three times. Then, the crude product was extracted by the method of Bligh and Dyer and used in the next step without further purification. *Rf* = 0.13 (chloroform/methanol/28% NH_3 solution = 65:25:4). ^{1}H-NMR (400 MHz, $CDCl_3$): δ 8.68-8.42 (br s, 2H), 5.48-5.26 (m, 10H), 4.15-4.04 (br s, 2H), 3.89-3.85 (m, 2H), 3.81-3.71 (m, 2H), 3.63-3.38 (m, 3H), 3.23-3.05 (br s, 2H), 2.88-2.76 (m, 8H), 2.12-2.02 (m, 4H), 1.60 (tt, 2H, *J* = 7.2 and 7.2), 1.43 (tt, 2H, *J* = 7.8 and 7.8), 0.97 (t, 3H, *J* = 7.5). ^{31}P-NMR (160 MHz, $CDCl_3$): δ 0.955. ESI-MS: 483.2 $[M-H]^-$ ($C_{25}H_{43}O_6PN$).

Compound **40**

Using a procedure similar to that described for the preparation of **14** except for the reaction temperature, compound **40** (7.1 mg, 11.2 μmol, 80%) was obtained. The reaction temperature was changed from room temperature to 0˚C for specific reaction between the amino group and NBD-F. *Rf* = 0.51 (chloroform/methanol/28% NH_3 solution = 65:25:4). ESI-MS: 631.6 $[M-H]^-$ ($C_{31}H_{45}O_8PN_4$).

Fluorescence microscopic analysis

Fluorescence images of the cells were obtained using an epifluorescence microscope (E6F-RFL equipped with ×100 oil objective; Plan Fluor, Nikon, Japan) with a super-high pressure mercury lamp (Nikon model HB-10103AF). Fluorescence filters, UV-1A (Ex: 365/10, DM: 400, BA: 400) and B-2A (Ex: 450-490, DM: 505, BA: 520), were used for Hoechst 33342 fluorescence (Ex: 350 nm, Em: 460 nm) and NBD fluorescence (Ex: 467 nm, Em: 540 nm), respectively. Digital images were acquired and analyzed using ImageJ software (http://rsbweb.nih.gov/ij/).

ESI-MS analysis of phospholipids

After the fluorescence microscopic analysis, lipids were extracted from the residual sample by the Bligh and Dyer method (2). Chloroform (100 μl) containing 1.14 μM 1,2-dilauroyl-*sn*-glycero-3-phosphoethanolamine (DLPE, Avanti Polar Lipids) as the internal standard 1 was used for the quantification of phospholipids. The chloroform-soluble fraction was dried, suspended in 100 μl of acetonitrile/methanol (2:1 v/v) containing 0.1% (v/v) ammonium formate (pH 6.5) and 1.02 μM 1,2-dipalmitoyl-*sn*-glycero-3-phosphoglycerol

(DPPG, Nippon Oil & Fats Co. Ltd) as the internal standard 2, and subjected to ESI-MS/MS analysis (Applied Biosystems API3000 LC/MS/MS system). Lipid samples (70 μl) were applied directly to the ESI source at a rate of 5 μl/min. The data were collected in the negative ion mode from 200 to 1200 m/z. The efficiency of lipid extraction was shown to be almost identical among samples by comparing the intensities of the internal standards 1 and 2. Experiments were repeated three times and yielded almost identical spectra. The fatty acyl residues in phospholipids were analyzed in the precursor ion scan mode. To compare the amounts of different NBD-labeled phospholipids incorporated into the cells, the following value was used:

$$A_{NBD}/A_{i.s.2}/I_{ef}/A_{600} \quad \text{-----(1)}$$

where A_{NBD} is an average area of the particular NBD-labeled phospholipid(s) in the mass spectra; $A_{i.s.2}$ is an average area of DPPG (internal standard 2) in the mass spectra; I_{ef} is the efficiency of lipid extraction, which was calculated by dividing "$A_{i.s.1}$ after extraction" by "$A_{i.s.1}$ before extraction," where $A_{i.s.1}$ is an average area of DLPE (internal standard 1) in the mass spectra; and A_{600} is the absorbance of the culture at 600 nm.

Dithionite assay for measuring lipid distribution in the inner (IM) and outer (OM) membranes

To determine the distribution of NBD-labeled phospholipids in the IM and OM of the bacterium, we employed a fluorescence-quenching assay by using sodium dithionite. Dithionite quenches NBD fluorescence by reduction and hardly penetrates across the lipid bilayer membrane because of its high hydrophilicity. Thus, dithionite can be used to determine the distribution of NBD-labeled phospholipids inside and outside the membrane

compartments (3-5). For this assay, we prepared the following three samples from *S. livingstonensis* Ac10 grown at 6°C in LB medium for 250 h: non-treated, lysozyme-treated, and lysozyme-and-Triton X-100-treated cells (Fig. S1A). Because both OM and IM are intact in non-treated cells, dithionite can access only the outer leaflet of OM (OM_{out}), where the fluorescence from the NBD-labeled phospholipids is quenched. When the cells are treated with lysozyme, the OM is disrupted, and both the inner leaflet of the OM (OM_{in}) and the outer leaflet of the IM (IM_{out}), in addition to the OM_{out}, become accessible to dithionite for fluorescence quenching. When the cells are treated with lysozyme and Triton X-100, both OM and IM are disrupted, and the inner leaflet of the IM (IM_{in}) as well as the OM_{out}, OM_{in}, and IM_{out} become accessible to dithionite for fluorescence quenching. To prepare the lysozyme-treated sample, 10 mg/ml of lysozyme in buffer A was added to the cells to the final concentration of 100 μg/ml, followed by the addition of 1.5 mM EDTA in buffer A to the final concentration of 0.5 mM. The sample was incubated on ice for 40 min. To prepare the lysozyme-and-Triton X-100-treated cells, 4% (w/v) Triton X-100 in buffer A was added to the lysozyme-treated sample to the final concentration of 0.4%, and the sample was incubated on ice for 20 min.

The assay was performed by the following procedure: (i) Cells incubated with NBD-labeled phospholipids for 250 h were diluted to A_{600} = 0.032 with buffer A (0.75M sucrose, 10 mM Tris-HCl (pH 7.5)) in a fluorescence cuvette. (ii) The fluorescence emission of this solution was recorded at an excitation wavelength of 467 nm and an emission wavelength of 540 nm by using a Hitachi 850S Fluorescence Spectrophotometer (Tokyo, Japan). (iii) After the fluorescence became constant, 1.0M of sodium dithionite ($Na_2S_2O_4$) in degassed H_2O was added at a final concentration of 10 mM, and the decrease in the

fluorescence was monitored. Experiments were repeated three times; each experiment yielded almost identical spectra.

Figure S1B shows a typical result of the dithionite assay obtained with the cells grown in the presence of Acylalkyl-EPA for 250 h. The degree of fluorescence quenching was in accordance with the degree of membrane disruption, verifying the validity of this method in determining the membrane localization of the NBD-labeled phospholipids. Each curve in Fig. S1B shows that the fluorescence intensity rapidly decreased in the initial stage of the reaction for about 2 min, and a very slow decrease of the fluorescence followed. The slow decrease is probably due to the slow passage of $S_2O_4^{2-}$ or SO_2^- radicals across the cell membranes and their reaction with NBD inside the membrane compartment (4). The slow reaction rate was extrapolated to time zero to determine the degree of "fast" fluorescence quenching corresponding to the reduction of the NBD group outside the membrane compartment.

To calculate the amount of NBD-labeled phospholipid inside the membrane compartment, which dithionite cannot access, the following equation was used:

Percentage of the NBD-labeled phospholipid inside the membrane = $(F_r - F_{ap})/(F_0 - F_{ap}) \times 100$ -----(2)

F_r is the fluorescence after the reaction with dithionite is complete, F_{ap} is the apparent fluorescence of the cells without NBD-labeled phospholipid, and F_0 is the fluorescence of the cells with NBD-labeled phospholipid before reaction. F_r is obtained by extrapolation of the slow reaction rate to time zero.

Fluorescence microscopic analysis of the cells treated with dithionite to

quench the fluorescence of NBD-labeled phospholipids in the OM_{out}

To find out on which membrane and on which side of the membrane the fluorescent NBD-labeled phospholipids were enriched after 250 h, we combined fluorescent microscopic analysis with the dithionite quenching method. The assay was performed by the following procedure: (i) *S. livingstonensis* Ac10 was cultivated in the presence of Acylalkyl-EPA and Lysoalkyl-EPA. The culture (200 μl each) was sampled at 250 h, and the cells were treated with Hoechst 33342 (final concentration = 25 μg/ml) for nucleoid labeling, followed by two wash with 200 μl of buffer A (0.75 M sucrose, 10 mM Tris-HCl (pH 7.5)). (ii) The cells were diluted to A_{600} = 2.7 with buffer A in a tube at 4°C. (iii) Sodium dithionite (100 mM) in degassed H_2O at 4°C was added to the suspension at a final concentration of 10 mM, and the mixture was incubated at 4°C. (iv) After 10 min of the incubation, the excess amount of dithionite was inactivated by the addition of 16% (v/v) of formaldehyde aqueous solution (methanol free). (v) Fluorescence images derived from NBD and Hoechst33342 of the cells were obtained using an epifluorescence microscope (E6F-RFL equipped with ×100 oil objective; Plan Fluor, Nikon, Japan). Digital images were acquired and analyzed using ImageJ software.

Legend to Scheme in Supplemental Data

Scheme S1

Synthetic scheme of NBD-labeled ether phospholipids, Dialkyl-EPA, Dialkyl-OLA, Acylalkyl-EPA, Acylalkyl-OLA, Methylalkyl-EPA and Lysoalkyl-EPA (compound **14**, **21**, **34**, **33**, **38**, and **40**, respectively). R_1COOH; oleic acid ($18:1_{9c}$), R_2COOH; eicosapentaenoic acid ($20:5_{5,8,11,14,17\ all\ cis}$). Reagents and conditions: a. $LiAlH_4$, THF, rt; b. methanesulfonyl chloride, triethylamine, benzene, rt; c. NaH, **5** (1.1 equiv.), DMSO, rt; d. $CHCl_3$/0.5 N HCl-MeOH (1:1, v/v); e. triphenylmethyl chloride, diisopropylethylamine, dichloromethane, rt; f. powdered KOH, **6** (1.0 equiv.), benzene, 40˚C; g. $POCl_3$, triethylamine, trichloroethylene-hexane (91:9, v/v), rt; h. 2-aminoethanol, triethylamine, THF, rt; i. 2-propanol-20% (v/v) AcOH aq. (2:1, v/v), rt; j. NBD-F, triethylamine, $CHCl_3$, rt; k. *p*-methoxybenzyl chloride, NaH, THF, 70˚C; l. NaH, **5** (2.0 equiv.), DMSO, rt; m. 2,3-dichloro-5,6-dicyano-*p*-benzoquinone, dichloromethane, rt; n. **1** (2.2 equiv.), dicyclohexylcarbodiimide, dimethylaminopyridine, $CHCl_3$, rt; o. iodomethane, NaH, THF, rt; p. PLA_1 (cat.), 1:5 (v/v) ether-aqua solution (50 mM sodium acetate (pH 4)), 35˚C; q. NBD-F, triethylamine, $CHCl_3$, 0˚C.

Legends to Figures in Supplemental Data

Fig. S1

Dithionite quenching assay. (*A*) Schematic diagram of the dithionite quenching assay to determine the distribution of NBD-labeled phospholipids in the IM and OM. Dithionite hardly penetrates across the lipid bilayer, thus quenching the NBD fluorescence only outside the membrane compartments. See text for details. (*B*) Typical result of the dithionite quenching assay for the cells grown in the presence of Acylalkyl-EPA. The assay was performed for the intact cells (*black*), the lysozyme-treated cells (*red*), and the lysozyme-and-TritonX-100-treated cells (*blue*). The dashed line is the extrapolation of the slow quenching curve to time zero. F_r is the intercept of the extrapolated line at time zero, indicating the fluorescence that should remain after fast quenching of the NBD fluorescence outside the membrane compartments.

Fig. S2

ESI-MS spectra of the phospholipids extracted from *S. livingstonensis* Ac10 grown in the presence of Diacyl-EPA (*A*) and Diacyl-OLA (*B*), in the negative ion scan mode. Spectra were measured after 36 h (purple), 60 h (blue), 105 h (green), 130 h (orange), and 166 h (red) of cultivation. Relative intensities of different samples were normalized by using the intensity of the internal standard (1,2-dilauroyl-*sn*-glycero-3-phosphoethanolamine). Phospholipids increased during cultivation were identified by MS/MS analysis (precursor ion scan and product ion scan) and are shown as X/Y-PE or –PG (X, Y = acyl chain, PE = phosphatidylethanolamine, and PG = phosphatidylglycerol).

References

1. Sato, S., Kurihara, T., Kawamoto, J., Hosokawa, M., Sato, S. B., and Esaki, N. (2008) *Extremophiles* **12,** 753-761
2. Bligh, E. G. and Dyer, W. J. (1959) *Can. J. Biochem. Physiol.* **37,** 911-917
3. Huijbregts, R. P., de Kroon, A. I., and de Kruijff, B. (1996) *Biochim. Biophys. Acta* **1280,** 41-50
4. McIntyre, J. C. and Sleight, R. G. (1991) *Biochemistry* **30,** 11819-11827
5. Angeletti, C. and Nichols, J. W. (1998) *Biochemistry* **37,** 15114-15119

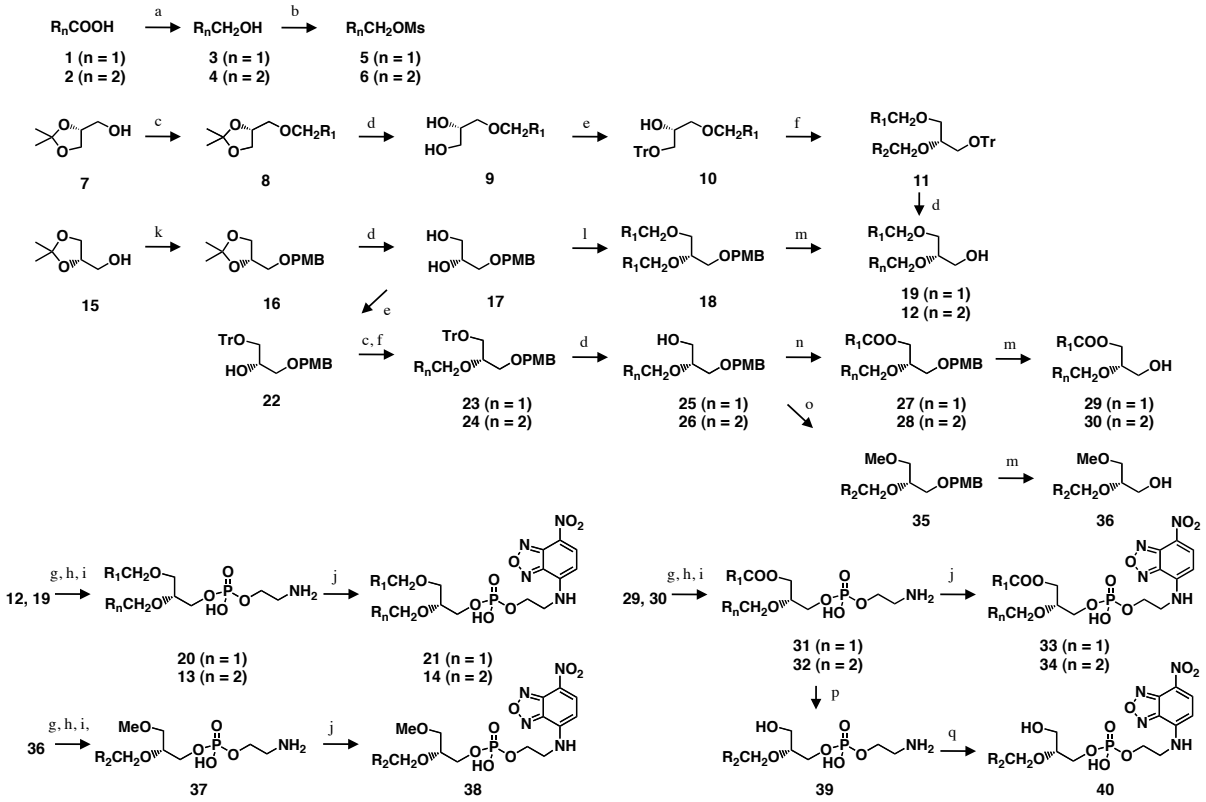

Scheme S1

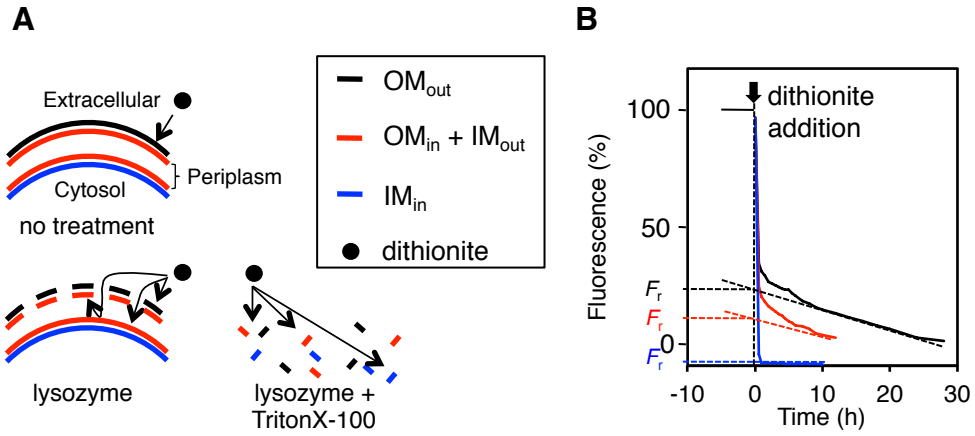
A
B
Extracellular
Periplasm
Cytosol
no treatment
lysozyme
lysozyme +
TritonX-100
OMout
OMin + IMout
IMin
dithionite
dithionite
addition
Fluorescence (%)
100
50
0
Fr
Fr
Fr
-10
0
10
20
30
Time (h)

Figure S1

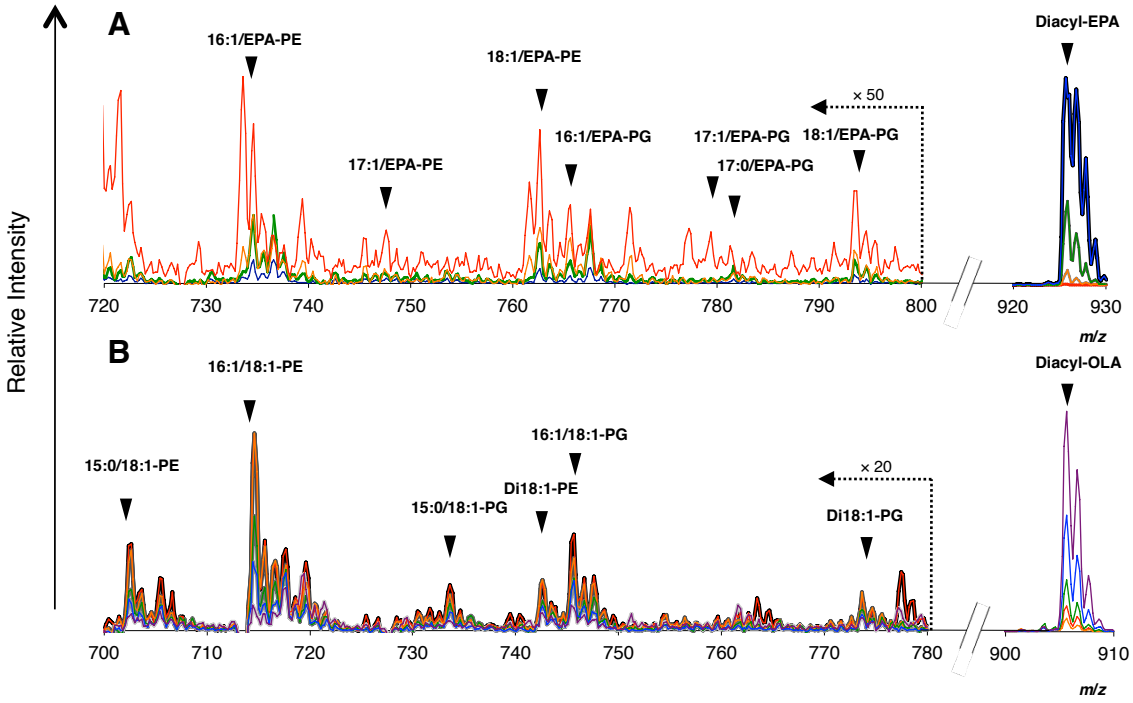
A
16:1/EPA-PE
18:1/EPA-PE
16:1/EPA-PG
17:1/EPA-PE
17:1/EPA-PG
18:1/EPA-PG
17:0/EPA-PG
× 50
Diacyl-EPA
Relative Intensity
720
730
740
750
760
770
780
790
800
920
930
m/z
B
16:1/18:1-PE
16:1/18:1-PG
15:0/18:1-PE
Di18:1-PE
15:0/18:1-PG
Di18:1-PG
× 20
Diacyl-OLA
700
710
720
730
740
750
760
770
780
900
910
m/z

Figure S2